NAVAL POSTGRADUATE SCHOOL
MONTEREY, CALIFORNIA

THESIS

A VALIDATION OF THE JOINT ARMY/NAVY
ROTORCRAFT ANALYSIS AND DESIGN
SOFTWARE BY COMPARISON WITH H-34 AND
UH-60A FLIGHT TEST

by

David M. Eccles

December, 1995

Thesis Advisor: E. Roberts Wood

Approved for public release; distribution is unlimited.

19960405 089

REPORT DOCUMENTATION PAGE

Form Approved OMB No. 0704-0188

1. AGENCY USE ONLY	2. REPORT DATE 1995, December	3. REPORT TYPE AND DATES COVERED Master's Thesis

4. TITLE AND SUBTITLE A VALIDATION OF THE JOINT ARMY/NAVY ROTORCRAFT ANALYSIS AND DESIGN SOFTWARE BY COMPARISON WITH H-34 AND UH-60A FLIGHT TEST	5. FUNDING NUMBERS
6. AUTHOR(S) Eccles, David M.	

7. PERFORMING ORGANIZATION NAME(S) AND ADDRESS(ES) Naval Postgraduate School Monterey CA 93943-5106	8. PERFORMING ORGANIZATION REPORT NUMBER
9. SPONSORING/MONITORING AGENCY NAME(S) AND ADDRESS(ES)	10. SPONSORING/MONITORING AGENCY REPORT NUMBER

11. SUPPLEMENTARY NOTES The views expressed in this thesis are those of the author and do not reflect the official policy or position of the Department of Defense or the U.S. Government.

12a. DISTRIBUTION/AVAILABILITY STATEMENT Approved for public release; distribution is unlimited.	12b. DISTRIBUTION CODE

13. ABSTRACT

A detailed comparison of the output from the NPS developed Joint Army/Navy Rotorcraft Analysis and Design (JANRAD) computer code with H-34 and UH-60A flight test data was made in an effort to determine the validity of the code's predictions. Airload distribution across the rotor disk, power required at various airspeeds ranging from hover to cruise, and thrust moment were used as measures of performance. Although a quantitative comparison of airload distribution is difficult to obtain, qualitatively, the predictions are good. JANRAD's power required estimations are correct to within two percent for altitudes below six thousand feet but accuracy suffers at higher altitudes, particularly above ten thousand feet. A correlation between the variation in kinematic viscosity from sea level to ten thousand feet and the accuracy of the power predictions is demonstrated. In the case of the UH-60A, the equivalent flat plate area of the helicopter is shown to be a function of airspeed, significantly impacting the accuracy of the power required prediction. Center of gravity offset from the main rotor's axis of rotation and unsteady inflow effects influence the accuracy of thrust moment predictions.

14. SUBJECT TERMS **Flight Test, JANRAD, Validation, H-34, UH-60, Rotorcraft**	15. NUMBER OF PAGES 83
	16. PRICE CODE

17. SECURITY CLASSIFICATION OF REPORT Unclassified	18. SECURITY CLASSIFICATION OF THIS PAGE Unclassified	19. SECURITY CLASSIFICATION OF ABSTRACT Unclassified	20. LIMITATION OF ABSTRACT UL

NSN 7540-01-280-5500

Standard Form 298 (Rev. 2-89)
Prescribed by ANSI Std. 239-18 298-102

A VALIDATION OF THE JOINT ARMY/NAVY
ROTORCRAFT ANALYSIS AND DESIGN SOFTWARE BY COMPARISON
WITH H-34 AND UH-60A FLIGHT TEST

David M. Eccles
Lieutenant , United States Navy
B.S.E.E., Tufts University, 1987

Submitted in partial fulfillment
of the requirements for the degree of

MASTER OF SCIENCE IN AERONAUTICAL ENGINEERING
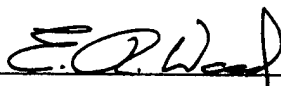
from the

NAVAL POSTGRADUATE SCHOOL
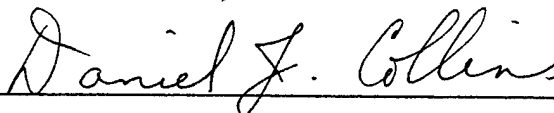**December, 1995**

Author: _____

David M. Eccles

Approved by: _____

E. Roberts Wood, Thesis Advisor

_____

S. K. Hebbar, Second Reader

_____

Daniel J. Collins, Chairman
Department of Aeronautical Engineering

iii

ABSTRACT

A detailed comparison of the output from the NPS developed Joint Army/Navy Rotorcraft Analysis and Design (JANRAD) computer code with H-34 and UH-60A flight test data was made in an effort to determine the validity of the code's predictions. Airload distribution across the rotor disk, power required at various airspeeds ranging from hover to cruise, and thrust moment were used as measures of performance. Although a quantitative comparison of airload distribution is difficult to obtain, qualitatively, the predictions are good. JANRAD's power required estimations are correct to within two percent for altitudes below six thousand feet but accuracy suffers at higher altitudes, particularly above ten thousand feet. A correlation between the variation in kinematic viscosity from sea level to ten thousand feet and the accuracy of the power predictions is demonstrated. In the case of the UH-60A, the equivalent flat plate area of the helicopter is shown to be a function of airspeed, significantly impacting the accuracy of the power required prediction. Center of gravity offset from the main rotor's axis of rotation and unsteady inflow effects influence the accuracy of thrust moment predictions.

DISCLAIMER

The views expressed in this thesis are those of the author and do not reflect the official policy or position of the Department of Defense or the U.S. Government

TABLE OF CONTENTS

I. INTRODUCTION

A. BACKGROUND

The Joint Army/Navy Rotorcraft Analysis and Design (JANRAD) computer code is a piece of software originally developed in 1993 by students at the Naval Postgraduate School (NPS) in Monterey California [Ref 1 and 2]. The code is intended to be used as a helicopter preliminary design tool. It is written in the Matrix Laboratory (MATLAB®) programming language, a high level language similar to FORTRAN but specifically designed to efficiently handle matrix operations. JANRAD, then, consists of a series of MATLAB® executable text files and requires that the user have access to a working copy of MATLAB®.

Since its initial distribution in 1993, JANRAD has gained a degree of popularity among aeronautical engineering students specializing in helicopters at NPS. The code has been used extensively by students participating in two nationwide helicopter design competitions sponsored by the American Helicopter Society as well as a variety of class projects. JANRAD has also been distributed to various organizations outside of NPS including divisions of the Naval Research Laboratory and NASA's Ames Research Center. Until recently, however, no dedicated effort to verify the validity of the code's output had been made. Such validation is the subject of this report.

B. METHODOLOGY

The methodology chosen to substantiate JANRAD's predictions involves developing a model of an existing helicopter for which detailed flight test data exists, running that model under JANRAD, and then comparing the code's output with the actual flight data. Emphasis is placed on validating the code with full scale flight test data versus wind tunnel test results or the output from other computer codes.

JANRAD is comprised of three primary modules; one for helicopter performance predictions, one for stability and control, and one for blade dynamics. The focus of this evaluation is on the performance module's ability to accurately predict three key parameters: the aerodynamic loading on the blades, main rotor power required throughout a wide range of airspeeds, and thrust moment. No effort is made to evaluate either the stability and control or blade dynamics modules. Another student has initiated an investigation of the stability and control portion as part of a separate report. The blade dynamics module is still under development and validation is yet premature.

Two sets of detailed airloads data presently exist in the United States. The first series of tests were conducted by NASA's Langley Research Center in 1964 using a Sikorsky H-34 Choctaw with an instrumented main rotor blade. The results of this project are published as NASA TM-X-952 [Ref 3], known to helicopter aerodynamicists as the Scheiman Report after its author. The second set of flight tests were completed more recently. In 1994, NASA's Ames Research Center concluded an extensive series of flight tests using a Sikorsky UH-60A Blackhawk. The raw data and many derived parameters from the Blackhawk tests reside in a computer database [Ref 4] presently maintained at the Ames Research Center. The amount of information contained in this database is on the order of 250 times that contained in Scheiman's work.

II. JANRAD

A. BASICS

JANRAD performs three separate tasks; performance prediction, stability and control analysis, and blade dynamics analysis. Each task is handled by a distinct module. The three modules are independent in that they do not call each other as sub-routines. However, the blade dynamics portion of JANRAD does use some of the performance module's results and requires that performance be run once first.

JANRAD's performance module and stability and control module are based on classical blade element theory. To determine the lift and drag on a main rotor blade, the blade is divided into a finite number of segments, or elements, and two dimensional (2-D) airfoil theory is applied to each element. Total lift and total drag on the blade is estimated by simply adding up the 2-D results from each individual blade element. Airflow near the blade's tip is dominated by three dimensional effects - most notably the tip vortex. Blade element theory handles this by defining a region near the tip in which only drag is considered.

The performance module "trims" the rotor by iteratively calculating, for a given set of flight conditions, rotor lift, rotor drag, and the location of the resultant thrust vector. The rotor's collective and cyclic pitch settings are adjusted until the rotor drag is within 20%, and the thrust vector within 1.5% of the previous iteration. When these parameters are met, the rotor is considered to be in trim. Performance module output includes main rotor power required, tail rotor power required, thrust moment, drag moment, and spanwise distributions of airload, induced velocity, and angle of attack.

The stability and control module calculates a set of linearized stability derivatives by perturbing the helicopter about its trim condition. The initial trim state is determined as described above for the performance module. If the helicopter is hovering (below 20 Kts), the

3

aircraft is trimmed, then its gross weight is increased by 0.5% and new trim conditions established. If the helicopter is in forward flight, the perturbation is about airspeed, +/- 0.05 %. Linearized stability derivatives are resolved based on variations in the trim state due to these perturbations.

The blade dynamics module uses the Myklestad -Thomson method to solve for the forced blade dynamic response. The code prompts the user for physical data related to the main rotor blades; specifically: mass distribution, flapwise stiffness distribution, chordwise stiffness distribution, root boundary condition, and lag damper damping coefficient. This module is still under development.

B. LIMITATIONS

Since JANRAD is based fundamentally on 2-D airfoil theory, the code exhibits some limitations. They are as follows. 1) Predictions are expected to be accurate in a hover and in forward flight at speeds greater than 50 kts where flow over the blades is relatively steady; the theory is invalid for the transition region from hover to forward flight. 2) JANRAD assumes steady inflow across the rotor. Blade vortex interaction, fuselage/rotor interference, and main/tail rotor interaction are not taken into account. 3) The code is based on the configuration of a conventional single main rotor helicopter, but can model winged compounds and circulation control anti-torque devices. 4) The aircraft's center of gravity is assumed to be located at the center of rotation of the main rotor for trimming. This eliminates the first harmonic term in thrust moment. 5) Lateral forces and moments due to the anti torque device and aerodynamic surfaces are ignored for the purposes of rotor trim. 6) The code is not configured to account for lift due to a canted tail rotor.

C. RECENT CHANGES

JANRAD is steadily being modified and its capabilities upgraded. The original edition

4

consisted of the performance and stability and control modules only. A third module to handle blade dynamics is currently under development by another student as a master's thesis project. Students have modified the performance routine by incorporating the Wheatley equation for forward flight, adding a section which allows the user to automatically iterate JANRAD over a range of useful parameters, and by working out a few minor bugs.

Other changes have also been incorporated as a result of this validation analysis. The original edition of JANRAD allowed the user to choose between two airfoils, the Boeing VR-12 and the McDonnell Douglas HH-02, both of which are cambered. The H-34 helicopter against which JANRAD is being compared, however, was outfitted with a NACA 0012 airfoil. In the interest of developing a more realistic model of the H-34, the NACA 0012 has been added as a new airfoil option. The NACA 0012 airfoil calculations were subsequently modified to account for compressibility effects. While JANRAD still calculates lift and drag coefficients for the VR-12 and HH-02 only as functions of local angle of attack, the calculations for the NACA airfoil are based on both local angle of attack and local Mach number. Appendix A contains the NACA 0012 MATLAB® code. JANRAD originally treated the tip loss region as a constant area. Wood, Kolar, and Cricelli (Ref 5) have shown that tip losses display a strong twice-per-revolution periodicity. Calculations involving tip losses have been revised so as to take into account the time varying nature of the tip loss region. Finally, the code has been adjusted so as to run smoothly under PC Windows® and UNIX® versions of MATLAB®. Appendix B is a listing of JANRAD files which ave been added or modified as a result of this thesis.

III. H-34 FLIGHT TEST

A. BACKGROUND

In the early 1960s, NASA's Langley Research Center conducted an extensive series of flight tests on a Sikorsky H-34 Choctaw helicopter. Figure 1 is an illustration of an H-34. Forty nine pressure transducers were installed in an otherwise production rotor blade. These transducers were connected to pressure taps in the upper and lower surfaces of the blade by twelve inch sections of plastic tubing at seven radial stations. Strain gages mounted on the blade's surface were used to determine flapwise and chordwise bending moment distributions. Blade root motions were measured using potentiometers attached to the cuff. Measurements were recorded at 15° rotor azimuth intervals for a total of 24 positions from $\Psi = 0°$ to 345°.
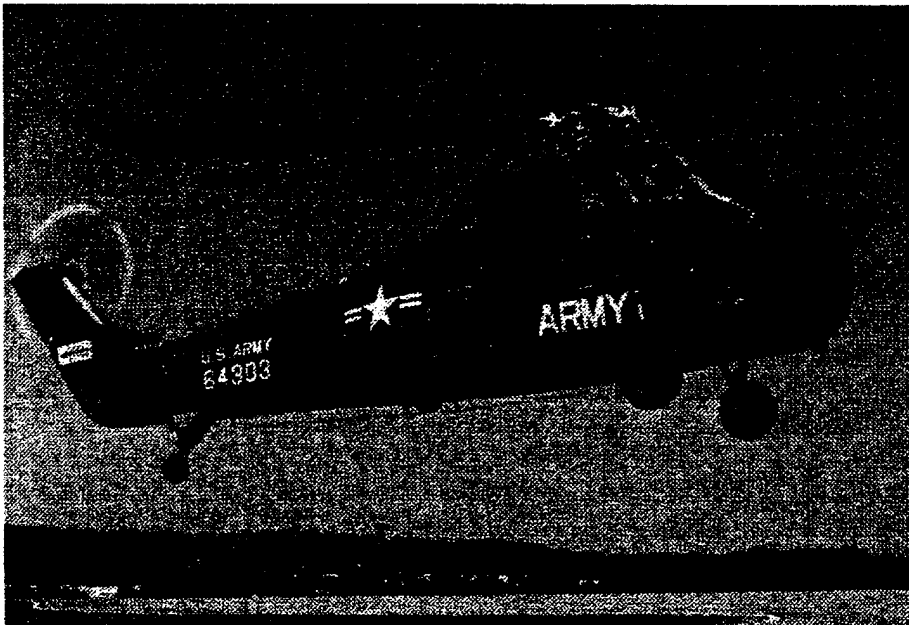

Figure 1. Sikorsky H-34 Choctaw.

The results of this flight test program were published in 1964 by James Scheiman [Ref 3]. Scheiman presents tabulated data for each of 94 flights. There are seven tables for each

flight: differential blade pressures, section aerodynamic loading, harmonic analysis of blade root motions, harmonic analysis of section aerodynamic loading, flapwise bending moment, chordwise bending moment, and blade torsional moment with pitch horn load. For steady flight conditions, pressure data from individual transducers was averaged over three rotor revolutions and then integrated chordwise at each blade radial station using Gauss's method of numerical integration. The resultant values of aerodynamic loading, in Lb/in, make up the bulk of the tabulated data used in this validation. Measurements of interest for this report were manually transcribed into MATLAB® ".m" files for comparison with JANRAD's output. Data were taken from three flights in particular: #1 (HOGE), #7 (56 KIAS), and #19 (115 KIAS).

B. DATA MANIPULATION

JANRAD's performance module output includes differential thrust calculated at each blade element and total thrust moment at each azimuth position. These outputs cannot be directly compared to Scheiman's tabulated data without some manipulation. Specifically, JANRAD's differential thrust was divided by the distance between blade elements to get airload in Lb/in. Total thrust moment was calculated from airloads tabulated in Scheiman's report. Thrust moment was determined by assuming the tabulated airload for a given pressure tap location was felt as a constant value by a section of blade ranging from points mid-way between pressure taps. Table 1 shows the pressure tap locations as a normalized radial stations, the blade length over which airloads from each tap were assumed to be effective, and the moment arm from the tap to the flapping hinge used in these calculations. The incremental thrust moments from each pressure tap location were summed to get the total moment. Thus, JANRAD's differential thrust was manipulated for comparison with Scheiman's airload, and Scheiman's airload was operated upon for comparison with JANRAD's thrust moment.

Recall the third key validation parameter is power required. The H-34 test aircraft was not configured to record a time history of rotor torque and Scheiman [Ref 3] indicates that there are unexplained inconsistencies when using the tabulated manifold pressures and rotor speeds

with H-34 engine characteristics to determine engine power output for the 1964 flights. For this reason it was decided not to attempt to validate JANRAD's predicted power required using H-34 data. Only UH-60A flight test data were used for the power analysis.

r/R	0.25	0.40	0.55	0.75	0.85	0.90	0.95
Effective Length (in)	109.2	50.4	42	50.4	16.8	16.8	16.8
Moment Arm (ft)	6	10.2	14.4	20	22.8	24.2	25.6

Table 1. Parameters for H-34 thrust moment calculations.

IV. UH-60A FLIGHT TEST

A. BACKGROUND

In 1994 NASA's Ames Research Center concluded a series of flight tests on a Sikorsky UH-60A Blackhawk similar to those conducted thirty years earlier at Langley on the H-34. Figure 2 is an illustration of a UH-60A. A total of 221 miniature pressure transducers were installed at nine radial locations on one main rotor blade and nine groups of accelerometers and strain gages were built into another. Measurements were recorded at 256 azimuth positions per revolution (about every 1.4°). Over 900 different flight conditions were explored.
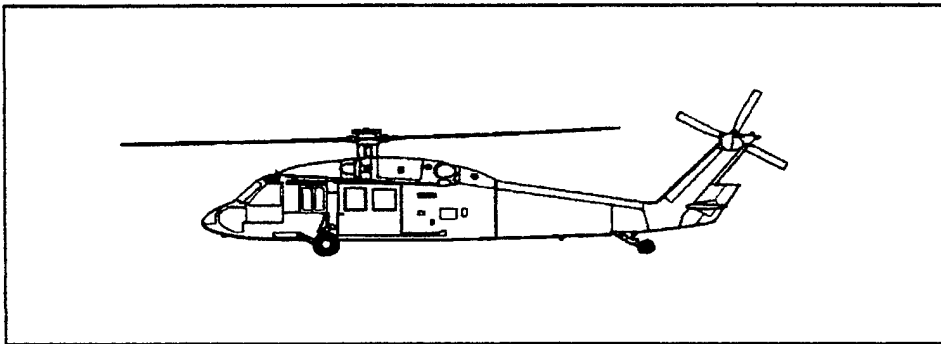
Figure 2. Sikorsky UH-60A Blackhawk.

The raw flight test data and a wide variety of derived parameters reside in a computer database presently maintained at the Ames Research Center. The Tilt Rotor Engineering Database System (TRENDS) [Ref 4] is an interactive relational database originally developed for the XV-15 program. The system has been expanded to support flight and wind tunnel tests of other rotorcraft including the UH-60A. After establishing a TRENDS account, straight and level flight data recorded on flights 84, 85, 88, 89, and 90 were simply downloaded via modem. Only minor reorganization was required to put the data in a format useful to MATLAB®. Appendix C contains instructions and copies of the required forms for starting an account on the TRENDS system.

11

B. DATA MANIPULATION

Data for the UH-60A portion of this analysis was manipulated in the same manner as for the H-34 portion. JANRAD's differential thrust was divided by the length of the blade elements to get airload in Lb/in. These values were compared with the recently derived parameter labeled CN in the TRENDS database. CN, in Lb/in, is the result of integrating the air pressures on the blade at a given radial station and azimuth position. It is equivalent to the airload values tabulated in Scheiman's report. Thus, for a given blade azimuth, TRENDS contains CN1 through CN9 corresponding to each of the nine radial stations at which pressure sensors were located. The TRENDS system allows the user to specify the number of rotor revolutions over which to average time history parameters like CN. The values used for this report were averaged over nine revolutions. Since CN is derived (actually integrated) from pressures sensed on the rotor blade and those pressures were recorded 256 times per revolution, TRENDS contains 256 sets of CN values - each corresponding to blade azimuth positions about 1.4° apart. In an effort to keep the flight test airloads plots seen later in this report relatively uncluttered and consistent with their JANRAD counterparts, only every fifth set on CN values was downloaded; about every 15° in azimuth.

Total thrust moment was determined from CN values taken from TRENDS. These calculations were made using the same assumptions as for the H-34 airload data. Table 2 shows the pressure tap locations as normalized radial stations, the blade length over which the CNs from each tap were assumed to be effective, and the moment arm from the tap to the flapping hinge used to compute thrust moment for the UH-60A. Rotor horsepower is a parameter common to both TRENDS and JANRAD. No manipulation of rotor power was necessary for comparison.

12

r/R	0.225	0.40	0.55	0.675	0.775	0.865	0.92	0.965	0.99
Effective Length (in)	64.40	52.32	44.27	36.22	30.59	23.34	16.10	11.27	4.02
Moment Arm (ft)	4.78	9.47	13.50	16.85	19.54	21.95	23.43	24.63	25.30

Table 2. Parameters for UH-60A thrust moment calculations.

V. RESULTS

A. INPUTS TO JANRAD

The first step in validating JANRAD was to develop software models of both the H-34 and the UH-60A. JANRAD's performance module accepts thirty five parameters as input. Appendices D and E detail the values used to build the JANRAD models. Some of these parameters, such as the number of main rotor blades, remained constant from one flight condition to another while others, pressure altitude for example, would necessarily change. Additionally, some approximations and assumptions had to be made. In particular, values of Cd_0 for the horizontal and vertical tail surfaces on both aircraft were assumed to be 0.01. Initial equivalent flat plate area and vertical projected area estimations were based on Prouty's treatment of these factors in his text [Ref 6]. The NACA 0012 was added to JANRAD's airfoil library in an effort to accurately model the H-34. Time constraints prevented the inclusion of the Sikorsky SC1095 and SC1095R8 airfoils installed on the UH-60A. Instead, the Blackhawk model used the VR-12 airfoil option already built into JANRAD. Twenty blade elements and twenty four azimuth sectors (fifteen degree segments) were chosen to provide reasonable resolution while keeping computation time within acceptable limits.

B. AIRLOADS

A quantitative comparison of airloads calculated from pressures measured in flight with JANRAD developed airloads is a tedious and, for the purposes of this project, essentially meaningless task. A rigorous quantitative analysis would involve determining the error between JANRAD's prediction and the observed value for each blade radial station and azimuth position at which measurements were taken. A statistical evaluation of these errors would result in a bunch of numbers whose real significance and bearing on reality would have been lost. It was decided, therefore, to review this data on a qualitative basis instead. Three flight conditions were examined for both the H-34 and UH-60A. They are: hover, forward flight near the

15

minimum power required airspeed (56 Kts for the H-34 and 65 Kts for the UH-60A), and forward flight at high speed (115 Kts for both helicopters).

Figures 9 and 10 in Appendix F are representations of the airload distribution around the rotor disk for an H-34 hovering out of ground effect (HOGE). By convention, rotor blade azimuth position Ψ has a value of zero when the blade is positioned over the tail of the fuselage. The rotor spins counterclockwise when viewed from above such that $\Psi = 90°$ over the right wing, $180°$ over the nose, and so on. In figures 9 and 10, $\Psi = 0°$ along the axis which extends from the center of the rotor to the lower left of the plot. Similarly, $\Psi = 90°$ along the axis which extends from the center of the rotor to the lower right. The fuselage is pointed, from tail to nose, from the lower left of the plot to the upper right. Airload, in pounds per inch, is measured along the vertical axis. The distance from a point on the plotted surface to the plane of the rotor, then, gives an indication of the loading on the blade at that point. The data used to construct figure 9 is taken from Scheiman [Ref 3]. Figure 10 is a complementary plot generated from JANRAD's output. The perspective and scale are the same for both pictures. These two figures portray in global terms how the aerodynamic loading varies across the rotor disk. It is important that the reader become familiar with the orientation of the rotor disk in these illustrations as a misunderstanding would surely lead to an incorrect interpretation of the results.

Figures 11 through 14 show the same data as the previous two figures in a more meaningful format for direct comparison between flight test values and JANRAD's prediction. Aerodynamic loading in pounds per inch is plotted against blade radial location with each plot representing a single azimuth position. The four figures are for $\Psi = 0°, 90°, 180°, $ and $270°$. JANRAD's approximation is accurate from the root to about 80% of the distance to the tip. Near the tip, however, JANRAD's model breaks down. Specifically, notice the sharp rise in airload near the tip in the flight data which is not represented in JANRAD's output. Figure 10 clearly shows the idealized nature of the model upon which JANRAD is based; there is no apparent variation in the predicted airload with azimuth position in a hover and the complex flow near the tip is not precisely modeled.

16

Figures 15 through 20 are similar to the previous six figures except that these represent data for an H-34 flying at 56 Kts. Figures 21 through 26 show similar information for the H-34 flying at 115 Kts. While correlation between flight and simulation is not exact, it is clear that JANRAD's airload distribution prediction does follow the general trends observed in flight. In particular, notice the reduction in airload on the advancing blade as the helicopter's speed increases. Also, observe how the airload distribution shifts out toward the tip on the retreating blade at higher speed; the result of the slow blade flying at high angle of attack. Figures 22 and 26 clearly show the presence of the reversed flow region on the left side of the rotor disk near the hub.

Figures 27 through 44 are a set of UH-60A airload distribution plots akin to those previously described for the H-34. All of the flight data presented in these figures is based on information taken from the TRENDS database. There are some important features in these illustrations worth noting. In figure 27, there is a distinct notch in the airload over the tail due to interference with the tail rotor and tail pylon. Figures 29 through 32 all show a dip in the airload between about 0.7 and 0.85 r/R - likely the result of blade vortex interaction. JANRAD does not model either of these effects. Notice also the sharp rise in airload above JANRAD's predictions near the blade tip at all azimuth positions in a hover. Recall a similar corona appeared in the H-34 hover plots. JANRAD's inability to correctly predict the tip airloads is directly related to the two dimensional nature of the blade element theory upon which the code is based.

C. POWER REQUIRED VS. AIRSPEED

Figures 45 through 48 are traces of actual and predicted main rotor power required versus airspeed for the UH-60A. Figure 45 presents data for flight 84, figure 46 for flight 85, figure 47 for flight 88, and figure 48 for flight 89. In all cases, the helicopter is in straight and level flight. The primary differences from flight to flight are that the helicopter's gross weight and the altitude at which the flights were flown both increased as the program progressed.

There are two noticeable "dents" in the "bucket" of the power required curves shown in figures 45 and 46. The first is between about 15 and 35 knots, the region in which the helicopter is transitioning from a hover to forward flight. The flow through the rotor in this speed regime is extremely complicated and is not accurately modeled by JANRAD. This is not unexpected, however; Nicholson acknowledges this limitation in his thesis [Ref 1] clearly stating that JANRAD is expected to be accurate in a hover (out of ground effect) and at speeds greater than 50 knots but not in the transition region between hover and forward flight.

A second less obvious dent appears between about 80 and 100 knots and is caused by variations in the helicopter's equivalent flat plate area as the stabilator position and fuselage pitch attitude change. During initial power required validation runs, equivalent flat plate area was held constant as an input parameter to JANRAD. None of the resulting curves predicted the slight increase in power required observed in the 80 to 100 knot region. Subsequent analysis led to the conclusion that equivalent flat plate area varies with airspeed and that this variation is due primarily to the position of the stabilator with respect to the airflow. Fuselage pitch attitude also contributes to changes in flat plate area, but to a much lesser extent. Figure 49 is a plot of fuselage pitch attitude and stabilator position versus airspeed for flight 85. The stabilator's position is displayed in terms of degrees "trailing edge down" with respect to the longitudinal axis of the fuselage while the fuselage pitch attitude is referenced to the horizon. For the purposes of the software model, equivalent flat plate area was estimated for four airspeed regimes. Table 3 is a summary of these regimes and the associated values of flat plate area used in the model.

Airspeed	0 to 50 Kts	50 to 90 Kts	90 to 140 Kts	140 to 160 Kts
Flat Plate Area	60 ft^2	55 ft^2	45 ft^2	50 ft^2

Table 3. Equivalent Flat Plate Area Values for the UH-60A Model.

While correlation between JANRAD and flight test for flights 84 and 85 is excellent,

accuracy of the code's prediction suffers for the later flights. This is due to JANRAD's inability to account for changes in the kinematic viscosity of the air with increased altitude. Flights 84 and 85 were flown in the vicinity of four to six thousand feet pressure altitude. Flights 88 and 89 were flown much higher; between nine and twelve thousand feet.

To understand how this difference in altitude influences the accuracy of JANRAD's output, it is appropriate to follow the steps the code takes to arrive at its solution. JANRAD determines its main rotor power requirements by first calculating the torque needed to keep the rotor spinning. This torque opposes the moment about the axis of rotation caused by drag on the rotor blades. The drag at each blade element is based on the value of the coefficient of drag output from the selected JANRAD airfoil file, either vr12clcd.m, hh02clcd.m, or 0012clcd.m. These files contain series of equations which are piecewise curve-fits of airfoil data taken during wind tunnel tests. Coefficient of drag is a function of Mach number, Reynolds number, and angle of attack. The airfoil files originally developed for JANRAD, vr12clcd.m and hh02clcd.m, estimate Cd as a function of angle of attack only. The equations which make up 0012clcd.m are functions of both angle of attack and Mach number. Reynolds number, which depends on kinematic viscosity is not taken into account. In essence, the information contained in JANRAD's airfoil files is only valid for the Reynolds numbers at which the wind tunnel tests (upon which the curve-fit equations are based) were conducted. Kinematic viscosity resides in the denominator of the expression for Reynolds number. As altitude increases, so too does kinematic viscosity. Thus the Reynolds number at which the rotor blades are flying decreases with altitude. Both Schlichting [Ref 7] and Prouty [Ref 6] illustrate that Cd increases with a decrease in Reynolds number. The bottom line here is that as the altitude at which a helicopter is flying increases, drag on the blades (for a given amount of lift) goes up causing the rotor to require more power to keep it flying and JANRAD does not model this phenomenon.

D. THRUST MOMENT

The third parameter used to validate JANRAD was thrust moment. Figures 50 through

19

55 are plots of actual and predicted thrust moment as it varies with rotor azimuth position. JANRAD's ability to accurately predict thrust moment depends greatly on airspeed. Notice the similarity in this trend between the H-34 plots and those for the UH-60A. Let us consider separately the three flight regimes explored in this study.

JANRAD's lack of precision in a hover is due to the location of the helicopter's center of gravity. The code assumes the center of gravity is located directly under the main rotor when trimming. This simplifying assumption eliminates the steady moment about the rotor hub due to an offset center of gravity in the coordinate system of the fuselage. Gerstenberger and Wood [Ref 8] discuss the relationship between moments in the rotating coordinate system of the rotor and the fixed coordinate system in which the fuselage resides. Specifically, the first harmonic terms in thrust moment in the rotating system transform into the steady moment in the fixed system. Since JANRAD eliminates the steady moment in the fixed coordinate system by locating the C.G. along the rotor's axis of rotation, the first harmonic term in thrust moment is also eliminated. In other words, there is no cyclic input required to counter the effect of an offset center of gravity. This is evidenced by how constant the predicted hover thrust moment is in figures 50 and 53.

As forward speed increases, flow through the rotor becomes increasingly less steady. One of JANRAD's fundamental assumptions is that the rotor's inflow is uniform, thus it is no great surprise that the thrust moment predictions illustrated in figures 51 and 54 do not closely resemble those observed in flight for similar conditions. The theory upon which the code is based simply does not apply. As airspeed increases further and the rotor's wake is left behind, the flow through the rotor begins to resemble uniform inflow again and the predominating cyclic input is that required to maintain the new trim condition. JANRAD's thrust moment approximation is correctly influenced by this cyclic input as seen in figures 52 and 55.

20

VI. CONCLUSIONS

This validation of JANRAD's performance module has served two purposes; the primary of which was to get a feel for how much trust a user can place in the code's output. The second result has been to highlight those parts of the code which would most benefit from improvement. JANRAD is a useful tool with some room for refinement.

The airloads plots in Appendix F clearly illustrate the sources of some of JANRAD's strengths and weaknesses. In particular, it is evident that three dimensional effects associated with the blade's tip vortices are at the root of many of the differences between predicted and observed spanwise airload distributions. By the same token, it is important to note that azimuthal variations in airload distribution with increased airspeed are accounted for fairly accurately. Future efforts to improve the precision of JANRAD's airload distribution predictions should concentrate on these tip effects.

The accuracy of JANRAD's power required calculations is very encouraging. This validation, however, has pointed out the significance of two factors, of which any future user of the code must be aware. First, variations in a helicopter's equivalent flat plate area with airspeed due to changing control surface positions and fuselage pitch attitude are critical to the accuracy of the power predictions. Second, JANRAD's power required calculations are sensitive to high pressure altitudes; predictions are most accurate for altitudes around five thousand feet and power estimates above ten thousand feet should be treated as suspect.

JANRAD's thrust moment predictions illustrate three key features. First, the assumption that the center of gravity is located under the main rotor significantly influences thrust moment estimates at low speed. This is evident in figures 50 and 53 where the code's output does not demonstrate the same periodicity observed in the flight data. Second, thrust moment predictions at slow speed are not particularly accurate. This is the result of JANRAD's fundamental assumption that the rotor's inflow is uniform. At slow speed, the inflow is not uniform and the

theory upon which JANRAD is based does not apply. Finally, JANRAD's thrust moment calculations begin to closely match the flight data at higher speeds. As the rotor's wake is left behind, flow through the rotor can again be approximated as uniform and the effects of cyclic input on thrust moment are properly reflected in the code's output.

VII. RECOMMENDATIONS

JANRAD's performance module relies heavily on the precision of the code's airload distribution prediction for many of its outputs. Future efforts to improve JANRAD should focus on eliminating or reducing the effects of limiting assumptions built into the code. There are five specific areas which would benefit from further attention. First, JANRAD's airfoil library is too small. It is an easy task to include a new airfoil into the code once the file containing the piecewise curve fits of Cl and Cd for that airfoil are written. There is some degree of work involved in developing those curve fits, however. Any future additions to the airfoil library should take compressibility effects (i.e. Mach number) into account. Prouty discusses compressibility effects and curve fitting techniques in his text [Ref 6].

Second, a scheme should be developed for taking into account the effects of flying at high altitudes. In particular, this validation has illustrated how variations in kinematic viscosity with altitude can influence JANRAD's ability to accurately predict required power. Two possible solutions to this problem come to mind. One involves developing a simple correction factor or scale and applying it as needed. The other involves rewriting the airfoil files such that Cl and Cd are treated as functions of angle of attack, Mach number, and Reynolds number. At present, JANRAD sees these coefficients as functions of only angle of attack for the HH-02 and VR-12 airfoils and as functions of angle of attack and Mach number for the NACA 0012. Since kinematic viscosity is one of the factors in Reynolds number, accounting for Reynolds number directly in the Cl and Cd calculations should solve the altitude problem. This technique, however, is more complicated and would likely have a significant impact on computation time.

Third, changes should be made to account for the effects of an offset center of gravity when trimming the rotor. JANRAD currently trims the rotor in a hover by assuming that there is no steady moment about the hub due to an offset center of gravity. The code could be modified by specifying a steady moment and having the code trim to a value other than zero. Fourth, the effects of the fundamental 2-D nature of the code could be reduced by developing a prescribed

23

wake or free wake analysis to better model 3-D and tip effects. Both prescribed wake and free wake techniques, however, would negatively impact computation time with free wake calculations taking an order of magnitude longer than prescribed wake. And finally, similar validation work should be completed on both the stability and control module and the blade dynamics module. Such efforts will doubtless lead to further suggestions for improving the code.

APPENDIX A. 0012CLCD.M

The following MATLAB ".m" file was added to JANRAD; the plots which follow are representative output. The figures are traces of Cl and Cd versus angle of attack. The first set is for a Mach number of 0.5 and the second set for a Mach number of 0.8.

```
% 0012clcd.m
%  oo12clcd calculates CL and CD for the NACA 0012
% airfoil given angle of attack in radians and the
% local Mach number:
%
% [CL,CD]=oo12clcd(alpha, Mach)
%
% Both 'alpha' and 'Mach' are intended to be vectors
% the elements of which correspond to the rotor blade
% radial stations of interest in a blade element analysis.
% All equations are based on Ray Prouty's treatment of
% the 0012 in his text.

function [CL,CD]=oo12clcd(alpha, Mach)
CL=zeros(size(alpha));
CD=zeros(size(alpha));
a=alpha*180/pi;
aL = 15 - 16.*Mach;
aD = 17 - 23.4.*Mach;
K1 = 0.0233 + 0.342.*(Mach.^7.15);
K2 = 2.05 - 0.95.*Mach;


% CL for Mach numbers < 0.725 and AOA inside +/- 20 deg:

chk=(Mach<0.725 & a>=0 & a<=aL);
 CL=CL+chk.*((0.1./sqrt(1-Mach.^2) - 0.01.*Mach).*a);

chk=(Mach<0.725 & a>aL & a<=20);
 CL=CL+chk.*((0.1./sqrt(1-Mach.^2) - 0.01.*Mach).*a - K1.*(a-aL).^K2);

chk=(Mach<0.725 & a>=-20 & a<-aL);
 CL=CL-chk.*((0.1./sqrt(1-Mach.^2) - 0.01.*Mach).*abs(a) - K1.*(abs(a)-aL).^K2);
```

```
chk=(Mach<0.725 & a>=-aL & a<0);
CL=CL-chk.*((0.1./sqrt(1-Mach.^2) - 0.01.*Mach).*abs(a));
```

% CL for Mach numbers > 0.725 and AOA inside +/- 20 deg:

```
chk=(Mach>=0.725 & a>=0 & a<=aL);
CL=CL+chk.*((0.677 - 0.744.*Mach).*a);
```

```
chk=(Mach>=0.725 & a>aL & a<=20);
CL=CL+chk.*((0.677 - 0.744.*Mach).*a - (0.0575-0.144.*(Mach-0.725).^0.44).*(a-aL).^(K2));
```

```
chk=(Mach>=0.725 & a<0 & a>=-aL);
CL=CL-chk.*((0.677 - 0.744.*Mach).*abs(a));
```

```
chk=(Mach>=0.725 & a<-aL & a>=-20);
CL=CL-chk.*((0.677 - 0.744.*Mach).*abs(a) -
(0.0575-0.144.*(Mach-0.725).^0.44).*(abs(a)-aL).^(K2));
```

% CL for all Mach numbers and AOA outside +/- 20deg:

```
chk=(a>20 & a<=161);
CL=CL+chk.*(1.15.*sin(2.*alpha));
```

```
chk=(a>161 & a<=173);
CL=CL+chk.*(-0.7);
```

```
chk=(a>173 & a<=180);
CL=CL+chk.*(0.1.*(a-180));
```

```
chk=(a>=-180 & a<=-173);
CL=CL+chk.*(0.1.*(a+180));
```

```
chk=(a>-173 & a<=-161);
CL=CL+chk.*(0.7);
```

```
chk=(a>-161 & a<-20);
CL=CL+chk.*(1.15.*sin(2.*alpha));
```

% CD for Mach numbers < 0.725 and AOA inside +/- 20 deg:

```
chk=(Mach<0.725 & a>=0 & a<=aD);
 CD=CD+chk.*(0.0081 + (-350.*a + 396.*a.^2 - 63.3.*a.^3 + 3.66.*a.^4).*10.^(-6));


chk=(Mach<0.725 & a>aD & a<=20);
 CD=CD+chk.*((0.0081 + (-350.*a + 396.*a.^2 - 63.3.*a.^3 + 3.66.*a.^4).*10.^(-6)) +
0.00066.*(a-aD).^2.54);


chk=(Mach<0.725 & a<0 & a>=-aD);
 CD=CD+chk.*(0.0081 + (-350.*abs(a) + 396.*a.^2 - 63.3.*abs(a).^3 + 3.66.*a.^4).*10.^(-6));



chk=(Mach<0.725 & a<-aD & a>=-20);
 CD=CD+chk.*((0.0081 + (-350.*abs(a) + 396.*a.^2 - 63.3.*abs(a).^3 + 3.66.*a.^4).*10.^(-6))
+ 0.00066.*(abs(a)-aD).^2.54);



% CD for Mach numbers > 0.725 and AOA inside +/- 20 deg:

chk=(Mach>=0.725 & a>=0 & a<=20);
 CD=CD+chk.*((0.0081 + (-350.*a + 396.*a.^2 - 63.3.*a.^3 + 3.66.*a.^4).*10.^(-6)) +
0.00035.*a.^2.54 + 21.*(Mach-0.725).^3.2);

chk=(Mach>=0.725 & a<0 & a>=-20);
 CD=CD+chk.*((0.0081 + (-350.*abs(a) + 396.*a.^2 - 63.3.*abs(a).^3 + 3.66.*a.^4).*10.^(-6))
+ 0.00035.*abs(a).^2.54 + 21.*(Mach-0.725).^3.2);



% CD for all Mach numbers and AOA outside +/- 20deg:

chk=(a>20 & a<=180);
 CD=CD+chk.*(1.03 - 1.02.*cos(2.*alpha));

chk=(a>=-180 & a<-20);
 CD=CD+chk.*(1.03 - 1.02.*cos(2.*alpha));
```
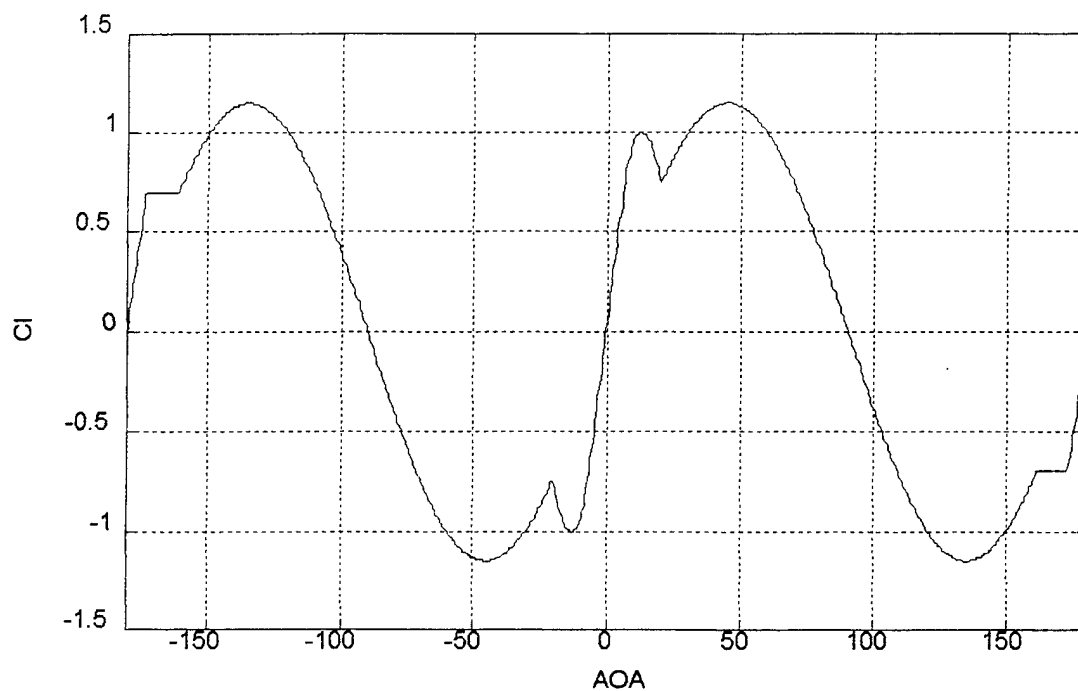
Figure 3. NACA 0012 at M = 0.5.
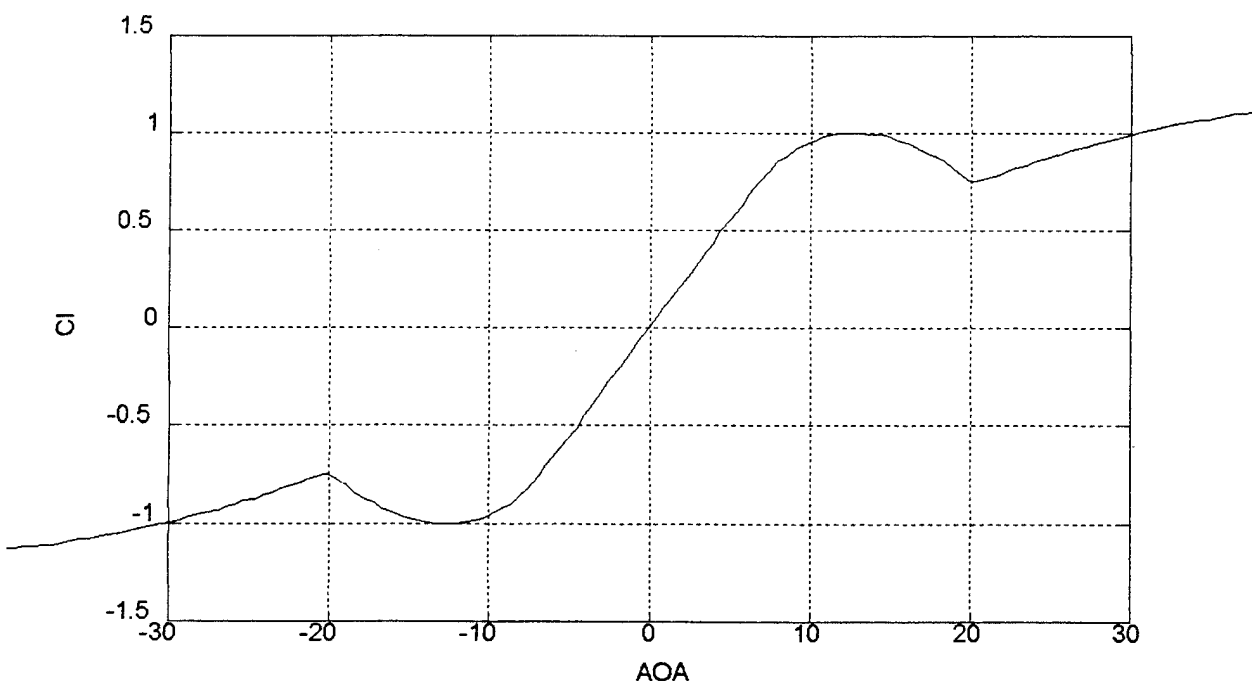
Figure 4. NACA 0012 at M = 0.5. (Note Different Scale)

28
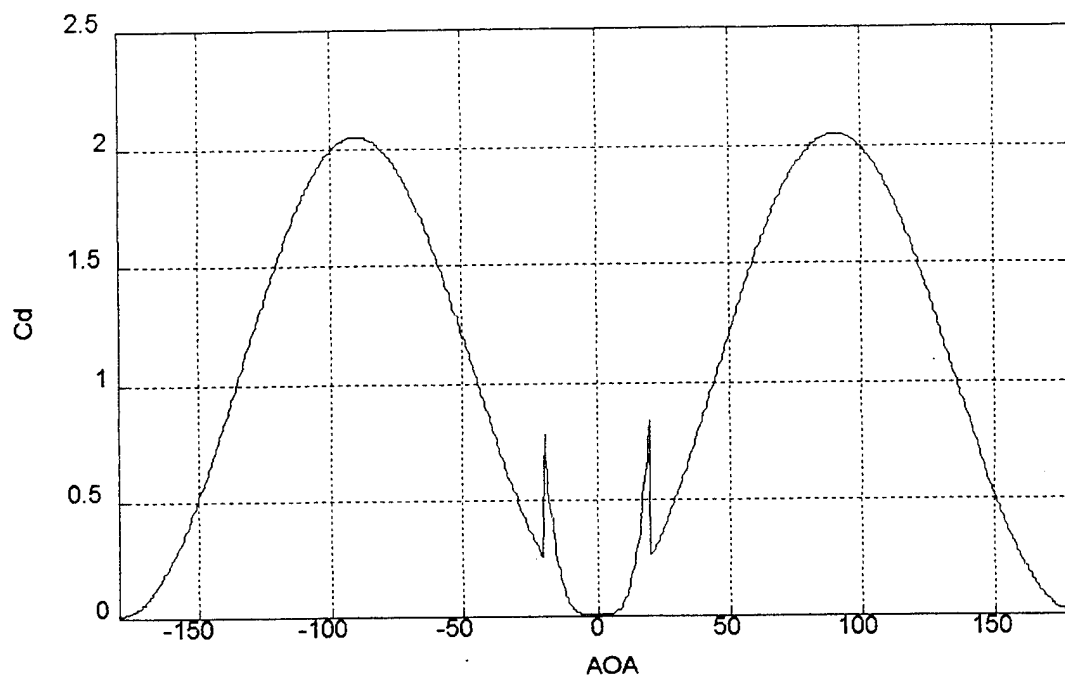
Figure 5. NACA 0012 at M = 0.5.
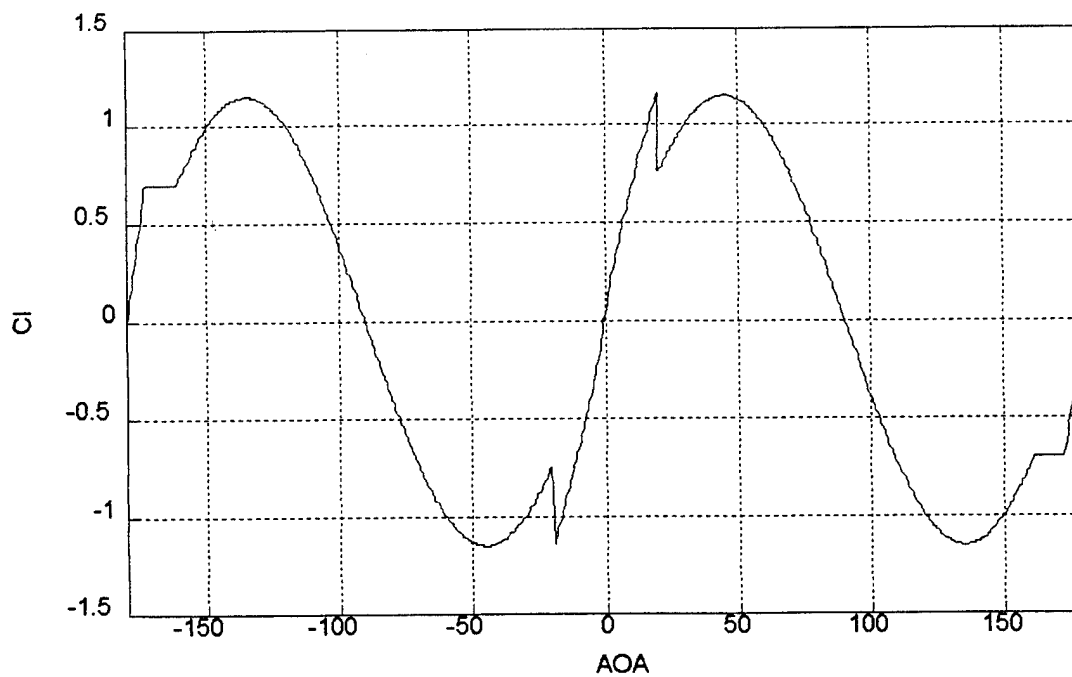
Figure 6. NACA 0012 at M = 0.8.
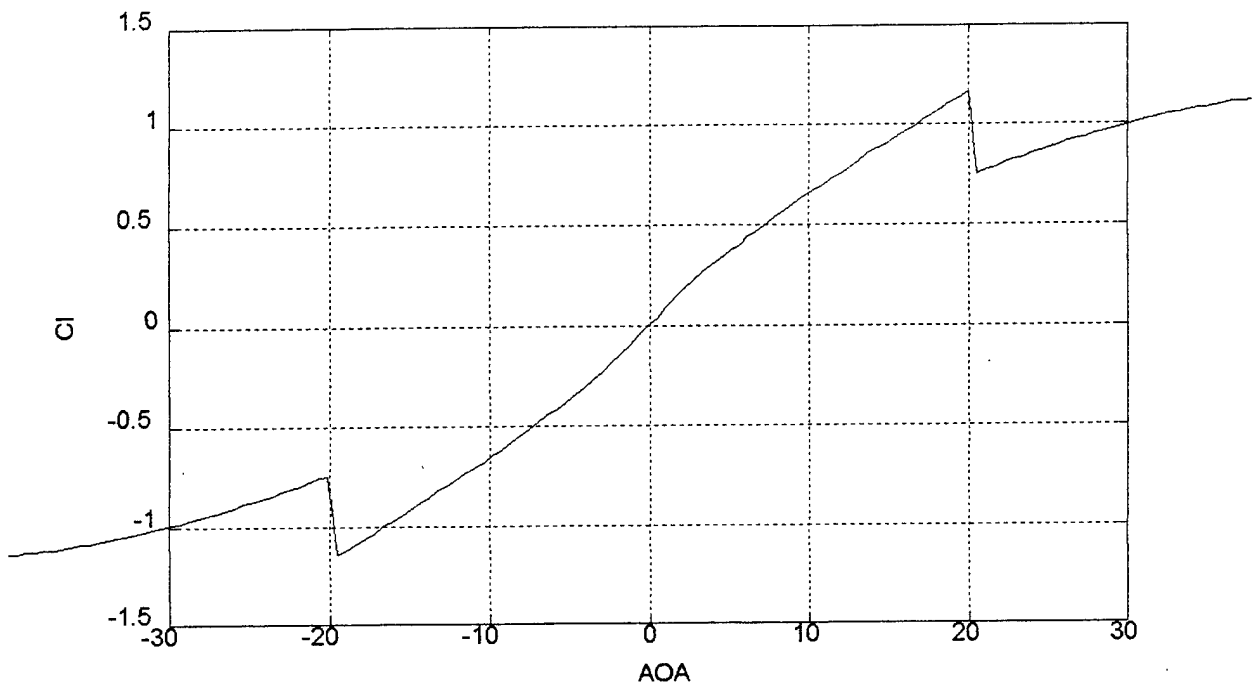
Figure 7. NACA 0012 at M = 0.8.   (Note Different Scale)
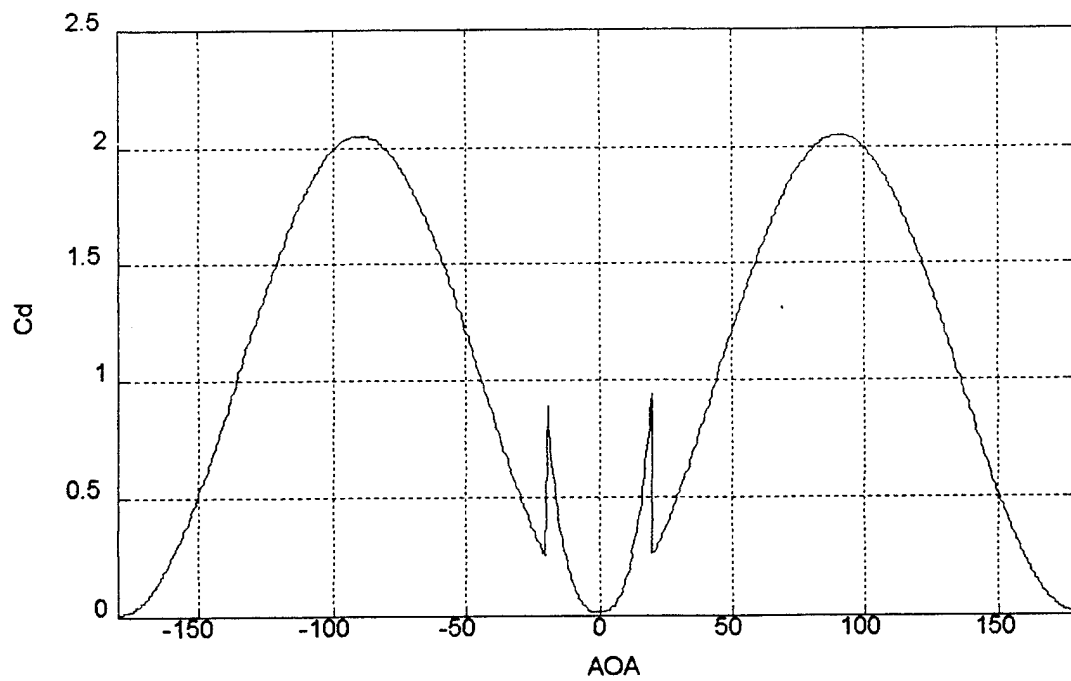
Figure 8. NACA 0012 at M = 0.8.

30

APPENDIX B.   LIST OF MODIFIED FILES

The following JANRAD files were modified from their original form:

dmcalc.m

janrad.m

oo12clcd.m

perf.m

stabout.m

thrcalc.m

tmcalc.m

APPENDIX C. ACCESS TO THE TRENDS DATABASE

The Tilt Rotor Engineering Database System (TRENDS) contains the raw data and many derived parameters from the Ames Research Center's UH-60A Blackhawk airloads flight test program. Access to this database is available to NPS students who hold U.S. citizenship. The following two pages are the forms necessary to apply for an account on the computer in which TRENDS resides and for access to the database itself. Prospective users are encouraged to photocopy these pages and submit them to the database manager. Mr. William G. Bousman is the primary point of contact; his address and telephone number are listed on the first form.

Request for USER ID on NEPtune VAX for
TRENDS Database System Usage

I would like to request an account to give me access to one of the NASA databases via TRENDS. I certify that data acquired through TRENDS shall not be disseminated to foreign companies or governments or their representatives without specific written authority by NASA.

I further understand that I will not publish any information using this data without written approval from William G. Bousman, MS T12-B, of NASA Ames. (415-604-3748)

Signature of Applicant _____

Applicable Contract or Grant Number (if any) _____

Data Base: XV-15   or   UH-60   I would like access because: _____

_____

_____

_____

_____

==

Requester's Name _____   _____
                                    Print   Date

COMPANY NAME & Address

_____

_____

_____

_____
                    Street, City, State, Zip Code

Telephone Number   _____   _____
                                    Area Code   Number

NASA Sponsor

    _____   _____
                    Signature/Phone   Date

Mail Form back to: William G. Bousman   Tel. 415-604-3748/FAX 415-604-1089
                              MS T12-B
                              NASA–Ames Research Center
                              Moffett Field, Calif.   94035-1000

NASA - Ames Research Center
Code FP - Aeronautical Projects Office
User Account Request and Authorization

FALSE OR INACCURATE INFORMATION PROVIDED ON THIS FORM IS A VIOLATION OF SECTION 499, TITLE 18, U.S. CODE *PLEASE PRINT or TYPE*	Complete items 1-11 and send form to: **Computer Systems Manager NASA Ames Research Center Mail Stop 237-2 Moffett Field, CA 94035-1000** You will be notified of account installation by FP Operations, (415) 604-6098.
1. Requestor Name (First, MI, Last): 3. Date:	2. Organization Name and Address:
4. Current/Previous FA Login Name:	5. Work Telephone:
6. Country of Citizenship:	7. If Non-U.S. Citizen, Provide Alien Registration Number (or Visa AND Passport Numbers):
8. Project Name:	
9. NASA Sponsor/Project Manager:	10. Sponsor/Project Manager's Signature:

I CERTIFY THAT MY FP COMPUTER ACCOUNT WILL BE USED ONLY BY MYSELF.

DIVULGENCE OF MY PASSWORD TO OTHERS WILL RESULT IN THE REMOVAL OF MY ACCOUNT.

NOTICE: Account deactivation will result after 90 days of non-use.

11. Requestor Signature: _____ Date: _____

Items 12 & 13 for FP Use Only

12. FP Authorizer's Signature: **Date:**

13 Authorized Access:

Items 12-17 for FP System Manager Use Only

14. Username:	15. UIC:
16. Account:	17. Device:
18. Directory:	19. Quota:
20. Remarks:	

Revised December 1993 (Previous Editions are Obsolete)

APPENDIX D. H-34 INPUT

1	Pressure Altitude [1]	4333 ft
2	Temperature [1]	68 F
3	Airspeed [1]	115 Kts
4	Gross Weight [1]	11500 lb
5	Number of Blades	4
6	Blade Radius	28 ft
7	Blade Root Chord	1.37 ft
8	Hinge Offset	1.0 ft
9	Blade Grip Length	3.5 ft
10	Blade Twist	-8.0 Deg
11	Blade Weight	175 lb
12	Number of Blade Elements	20
13	Rotational Velocity	24.19 Rad/s
14	Number of Azimuth Sectors	24
15	Lift Curve Slope	5.73
16	Airfoil	NACA 0012
17	Collective Pitch [2]	10 Deg
18	Flatplate Area [3]	35 ft^2
19	Vertical Projected Area [3]	227.5 ft^2
20	Wing Area	0
21	Wing Span	0
22	Wing Cl	0
23	Wing Cd_0	0
24	Wing Efficiency Factor	0
25	Horizontal Tail Area	9.0 ft^2

26	Horizontal Tail Span	6.0 ft
27	Horizontal Tail Cl [3]	-0.2
28	Horizontal Tail Cd_0 [3]	0.01
29	Vertical Tail Area	33 ft^2
30	Vertical Tail Span	8.5 ft
31	Vertical Tail Cl [3]	0
32	Vertical Tail Cd_0 [3]	0.01
33	Auxiliary Thrust	0
34	Rotor Blade Taper Ratio	1
35	Start of Taper	0

Notes: 1. These values varied from flight to flight; those shown are representative.

2. This value is only used as a starting point for the trim iteration.

3. These values are estimates.

APPENDIX E. UH-60A INPUT

1	Pressure Altitude [1]	3223 ft
2	Temperature [1]	69 F
3	Airspeed [1]	115 Kts
4	Gross Weight [1]	17377 lb
5	Number of Blades	4
6	Blade Radius	26.833 ft
7	Blade Root Chord	1.73 ft
8	Hinge Offset	1.26 ft
9	Blade Grip Length	3 ft
10	Blade Twist [2]	-18 Deg
11	Blade Weight	175 lb
12	# of Blade Elements	20
13	Rotational Velocity	26.4679 Rad/s
14	# of Azimuth Sectors	24
15	Lift Curve Slope	5.73
16	Airfoil	VR - 12
17	Collective Pitch [3]	10 Deg
18	Flatplate Area [1,4]	45 ft^2
19	Vertical Projected Area [4]	227.5 ft^2
20	Wing Area	0
21	Wing Span	0
22	Wing Cl	0
23	Wing Cd$_0$	0
24	Wing Efficiency Factor	0
25	Horizontal Tail Area	45 ft^2

26	Horizontal Tail Span	14.3833 ft
27	Horizontal Tail Cl [4]	0.8
28	Horizontal Tail Cd_0 [4]	0.01
29	Vertical Tail Area	32.3 ft^2
30	Vertical Tail Span	8.1667 ft
31	Vertical Tail Cl [4]	0
32	Vertical Tail Cd_0 [4]	0.01
33	Auxiliary Thrust	0
34	Rotor Blade Taper Ratio	1
35	Start of Taper	0

Notes: 1. These values varied from flight to flight; those shown are representative.

2. Equivalent linear twist.

3. This value is only used as a starting point for the trim iteration.

4. These values are estimates.

Figure 9. H-34 HOGE Airload Distribution - Flight
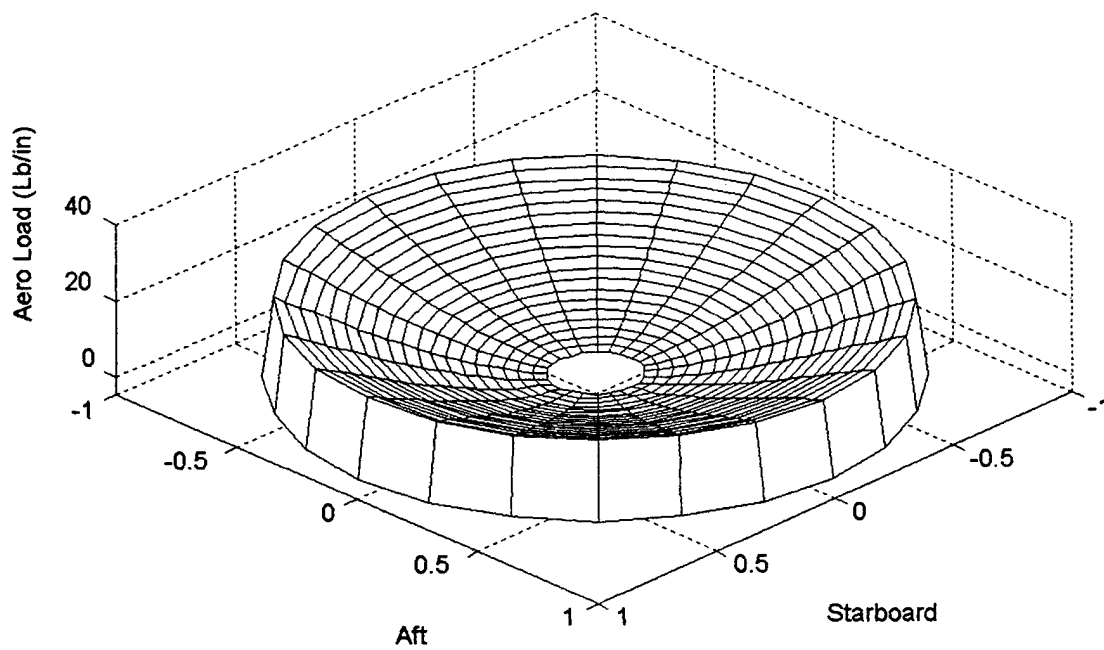
Figure 10. H-34 HOGE Airload Distribution - JANRAD
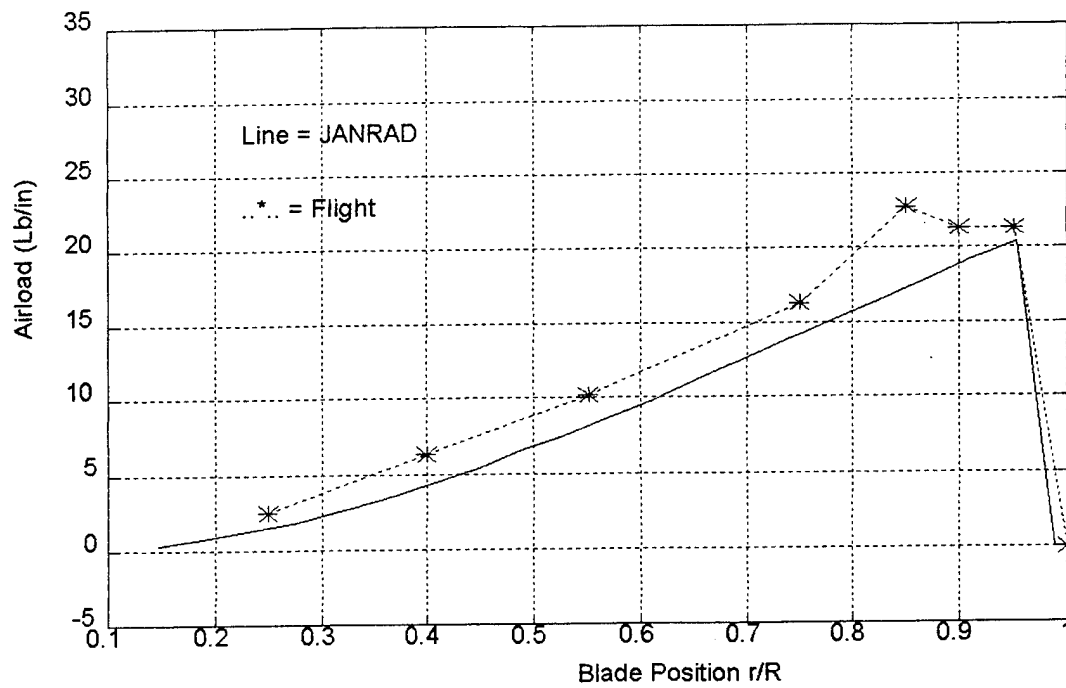
Figure 11. H-34 Radial Airload Distribution, HOGE, $\Psi = 0°$.
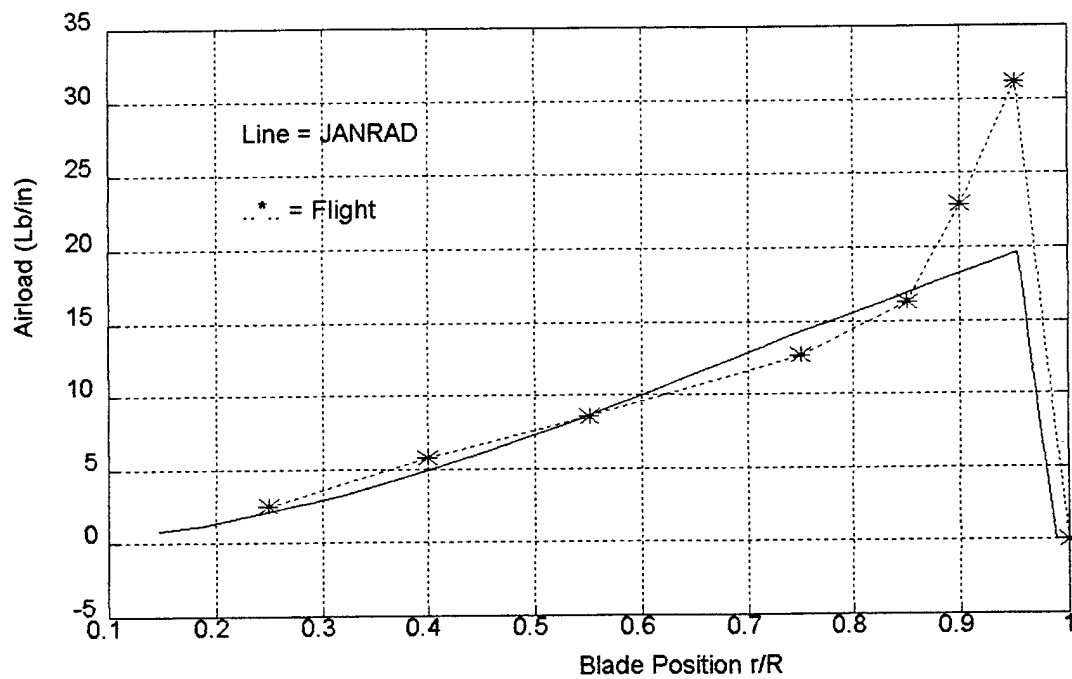
Figure 12. H-34 Radial Airload Distribution, HOGE, $\Psi = 90°$.

42
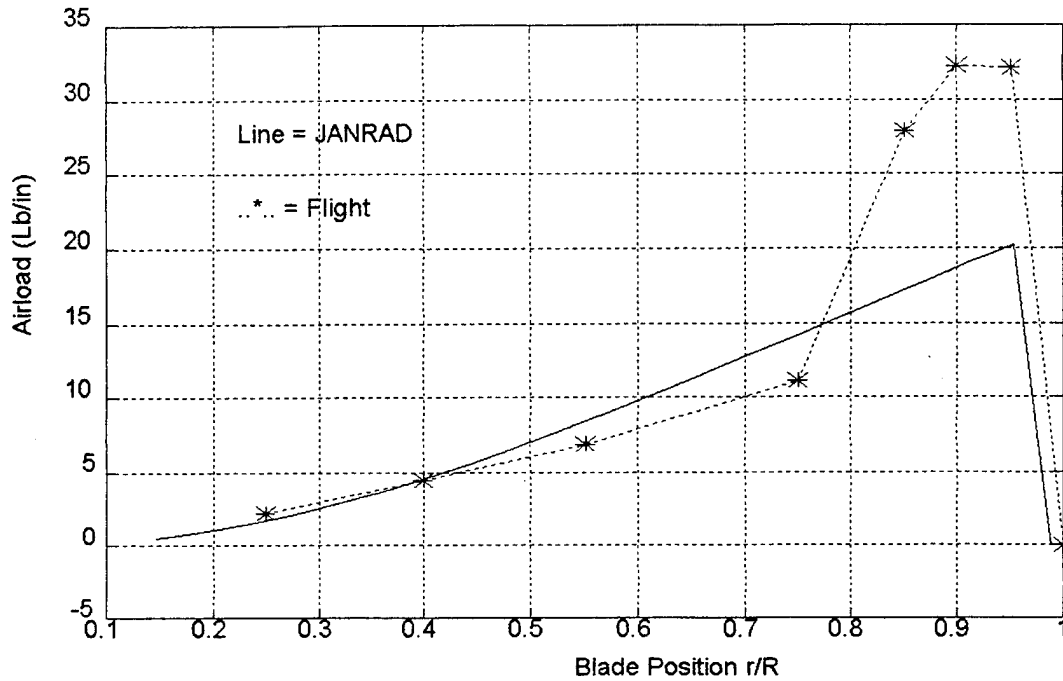
Figure 13. H-34 Radial Airload Distribution, HOGE, $\Psi = 180°$.
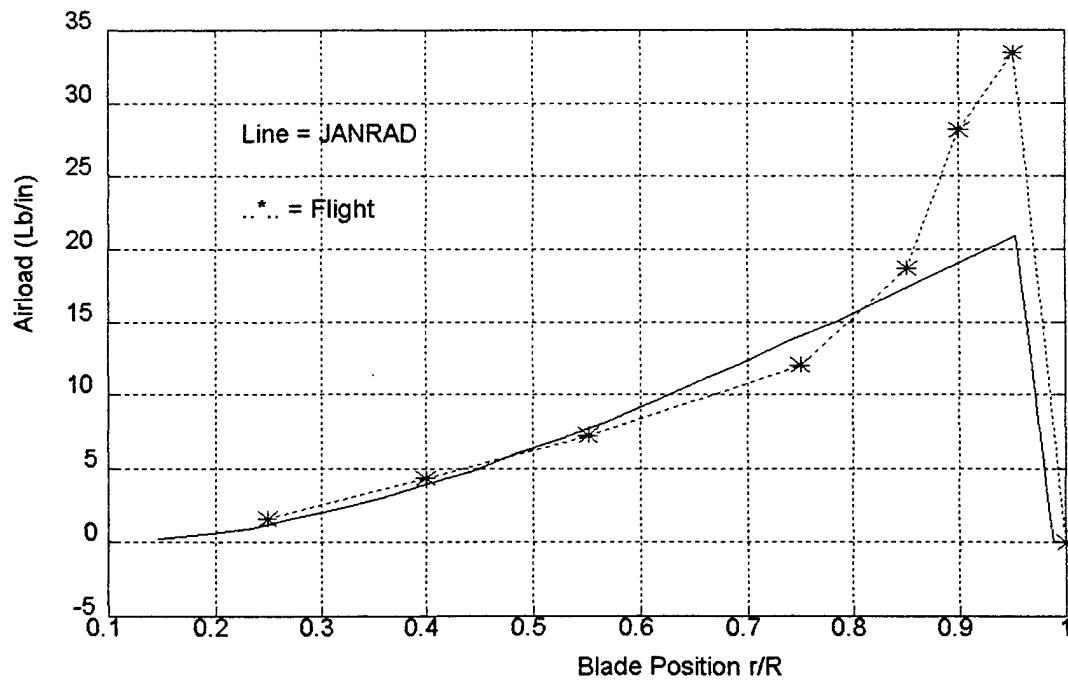
Figure 14. H-34 Radial Airload Distribution, HOGE, $\Psi = 270°$.

43
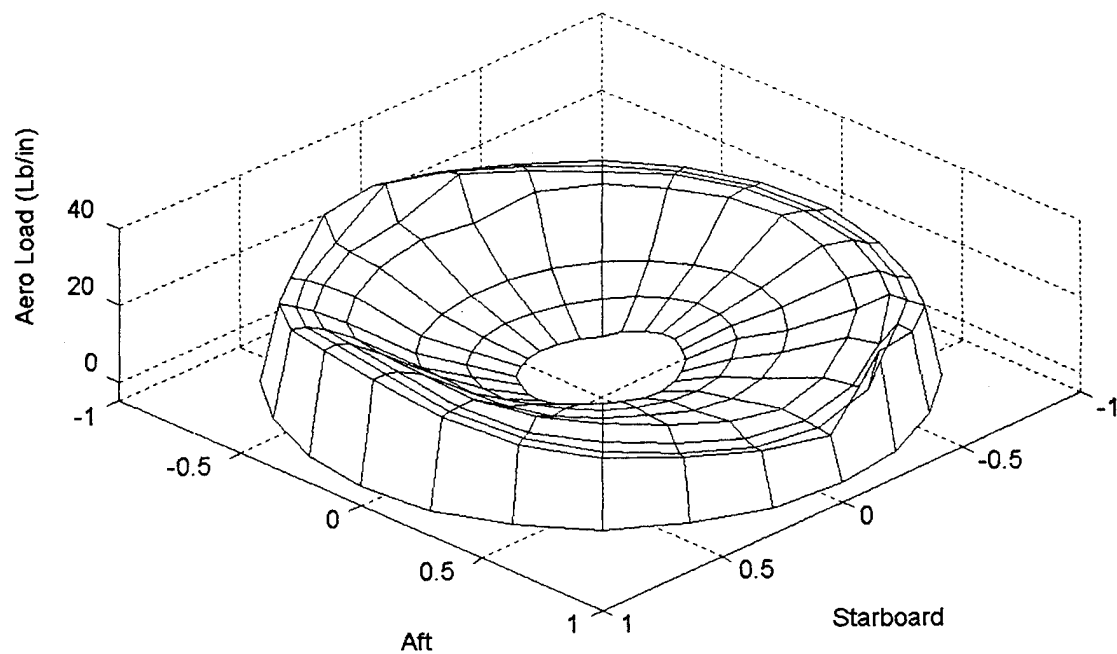
Figure 15. H-34 Airload Distribution at 56 Kts - Flight.
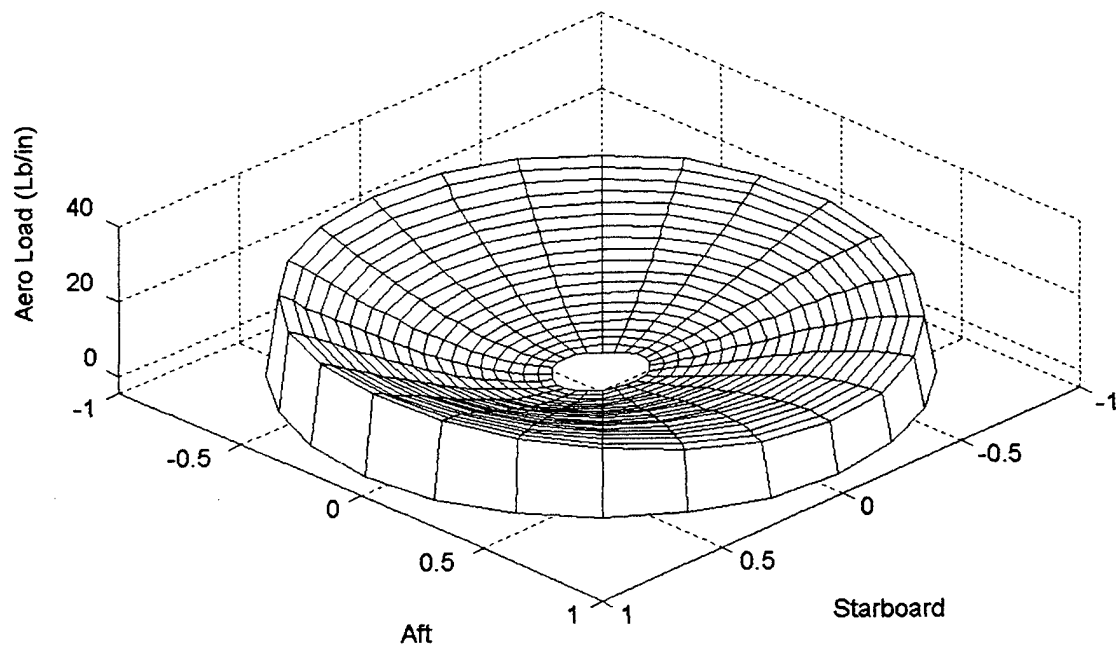
Figure 16. H-34 Airload Distribution at 56 Kts - JANRAD
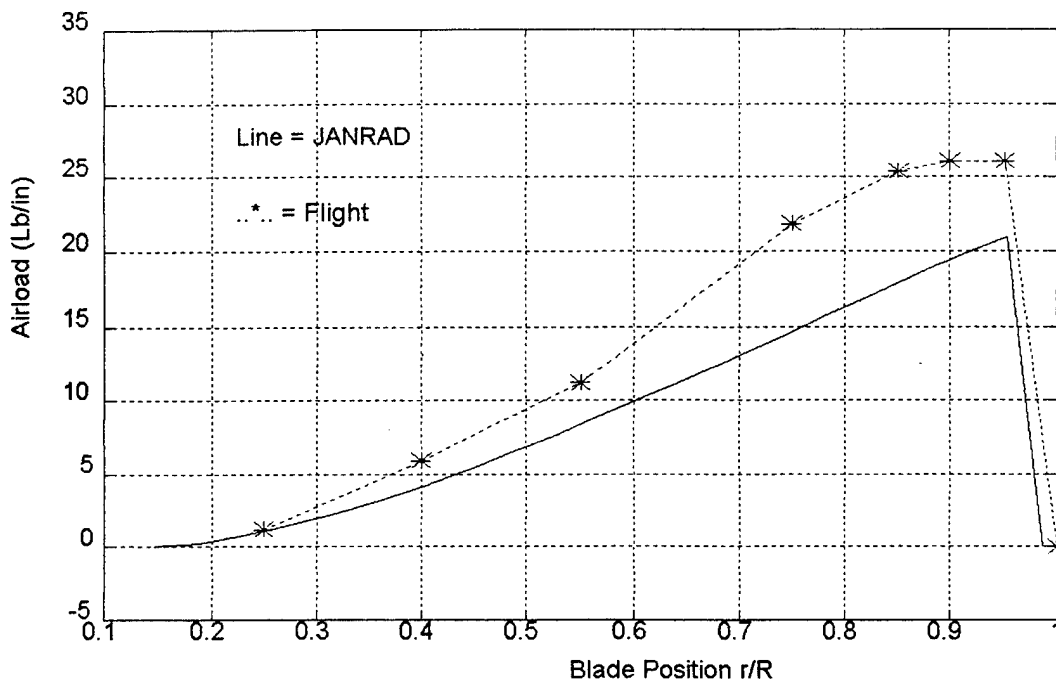
Figure 17. H-34 Radial Airload Distribution at 56 Kts, $\Psi = 0^\circ$.
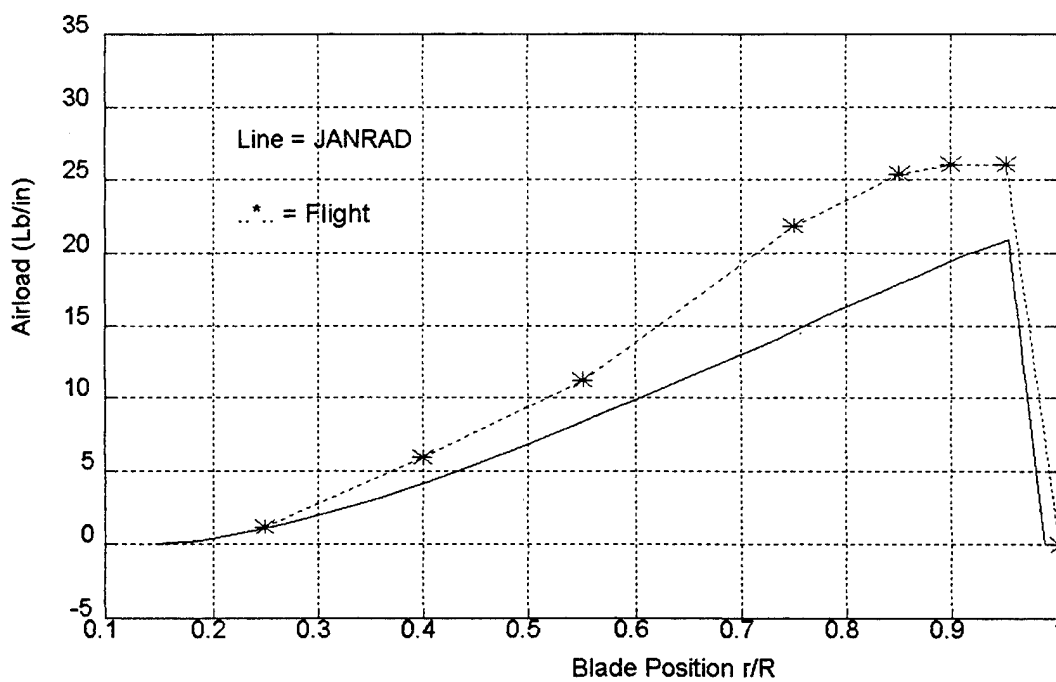
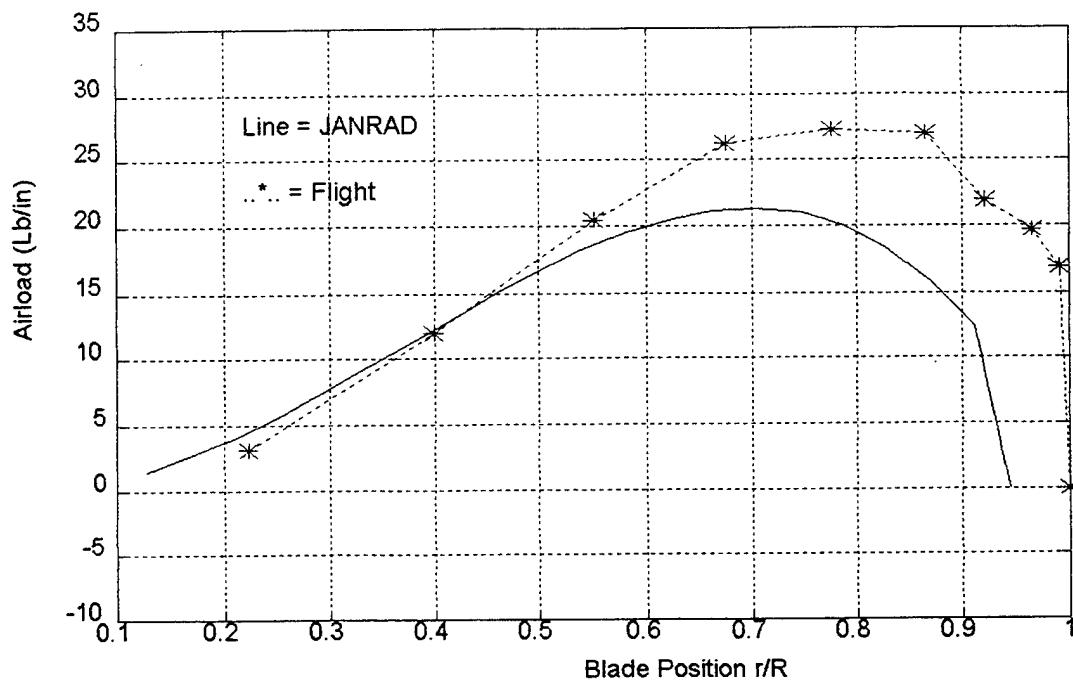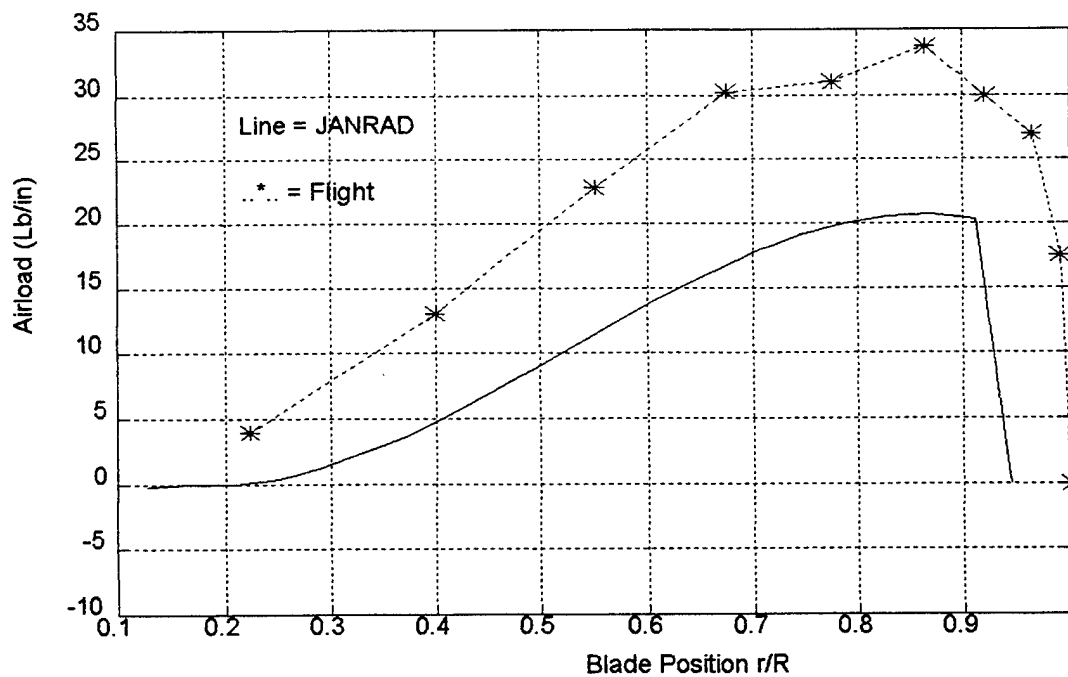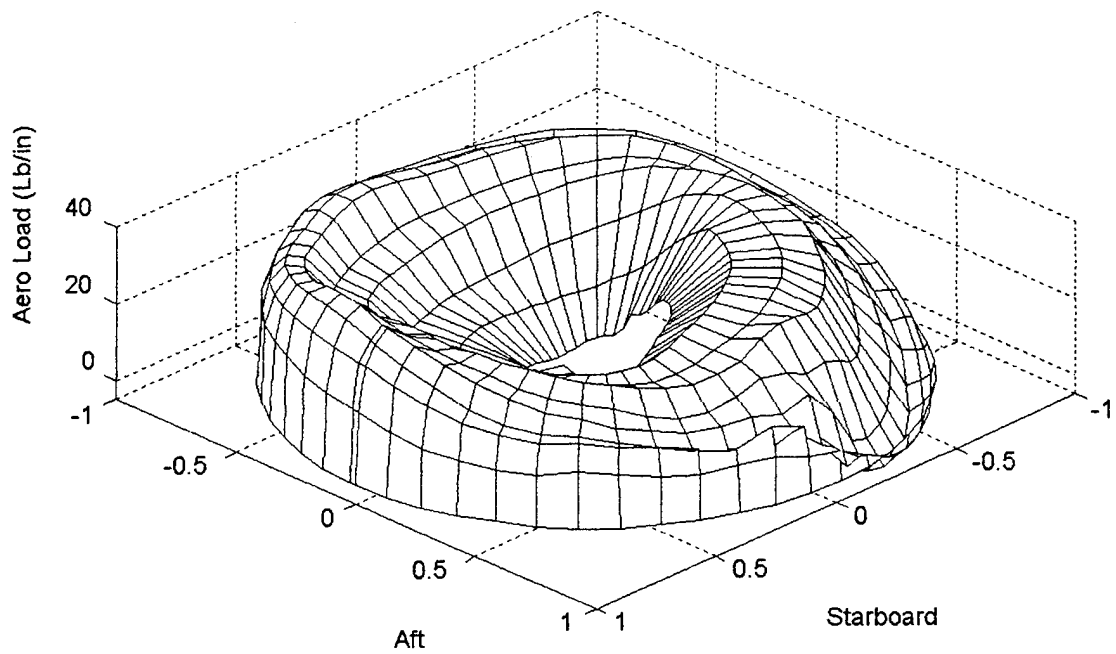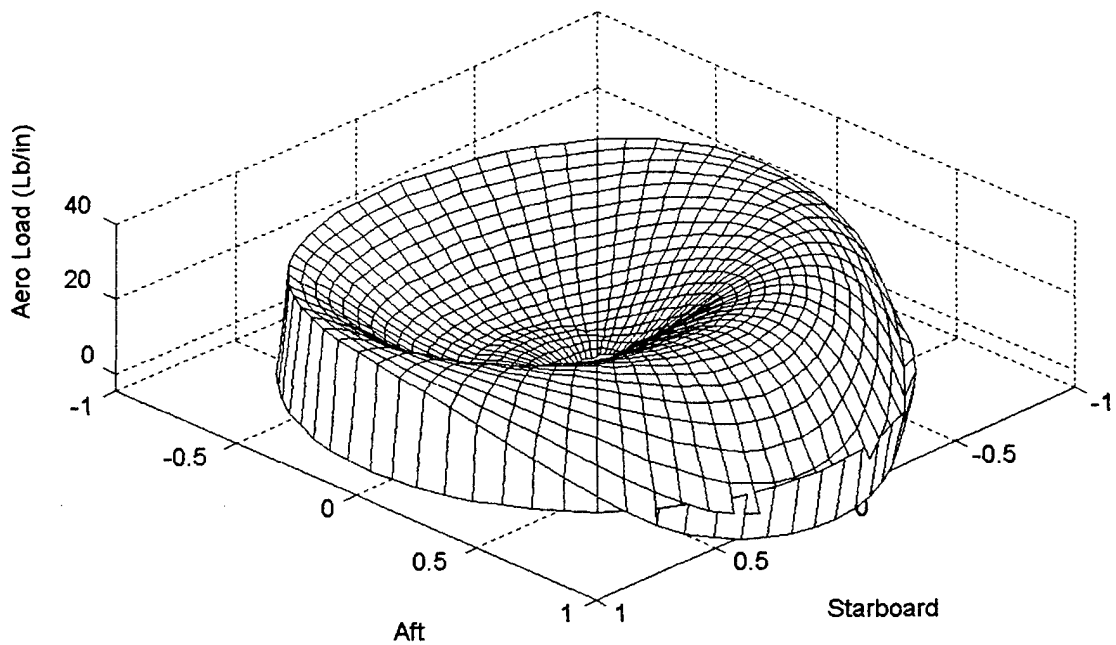**Figure 18.** H-34 Radial Airload Distribution at 56 Kts, $\Psi = 90^\circ$.

45
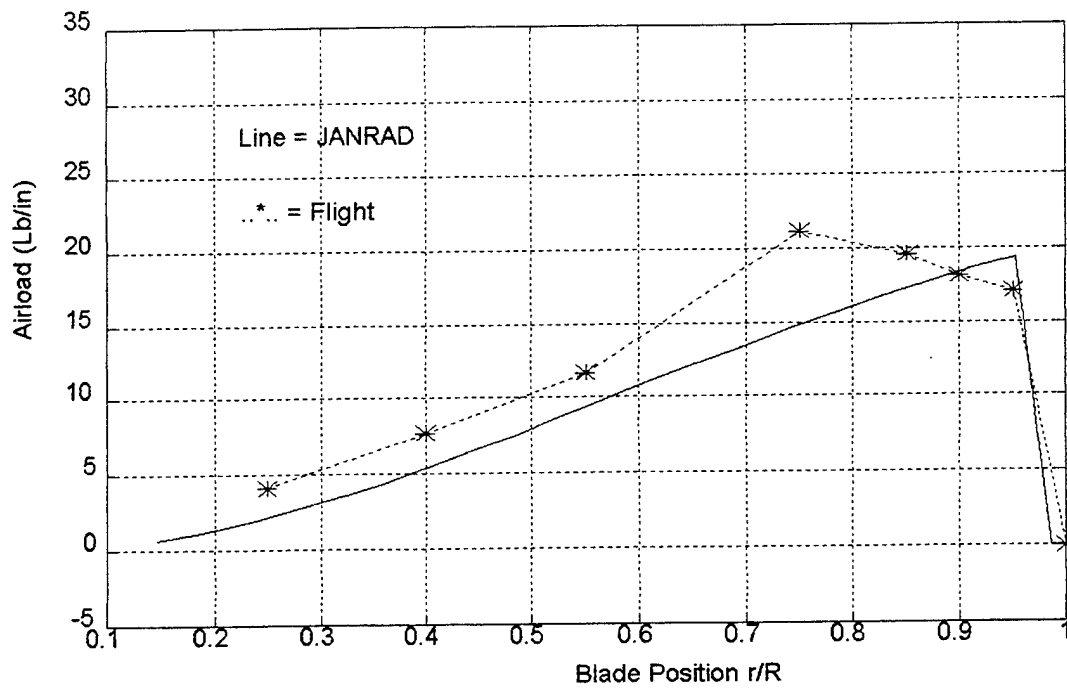
Figure 19. H-34 Radial Airload Distribution at 56 Kts, $\Psi = 180°$.
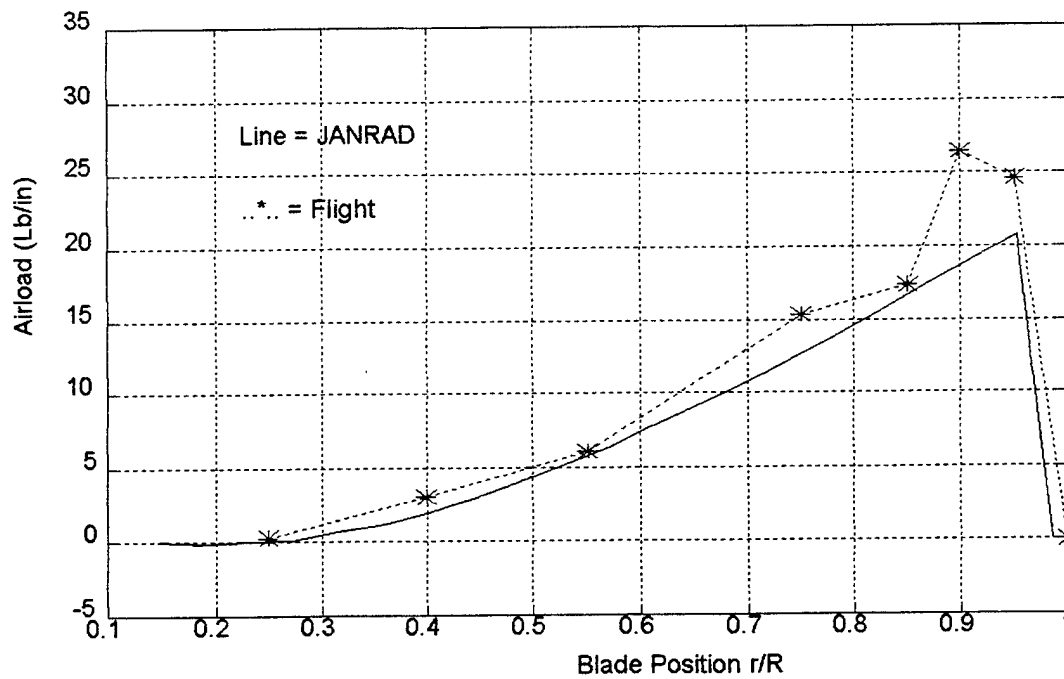
Figure 20. H-34 Radial Airload Distribution at 56 Kts, $\Psi = 270°$.

46
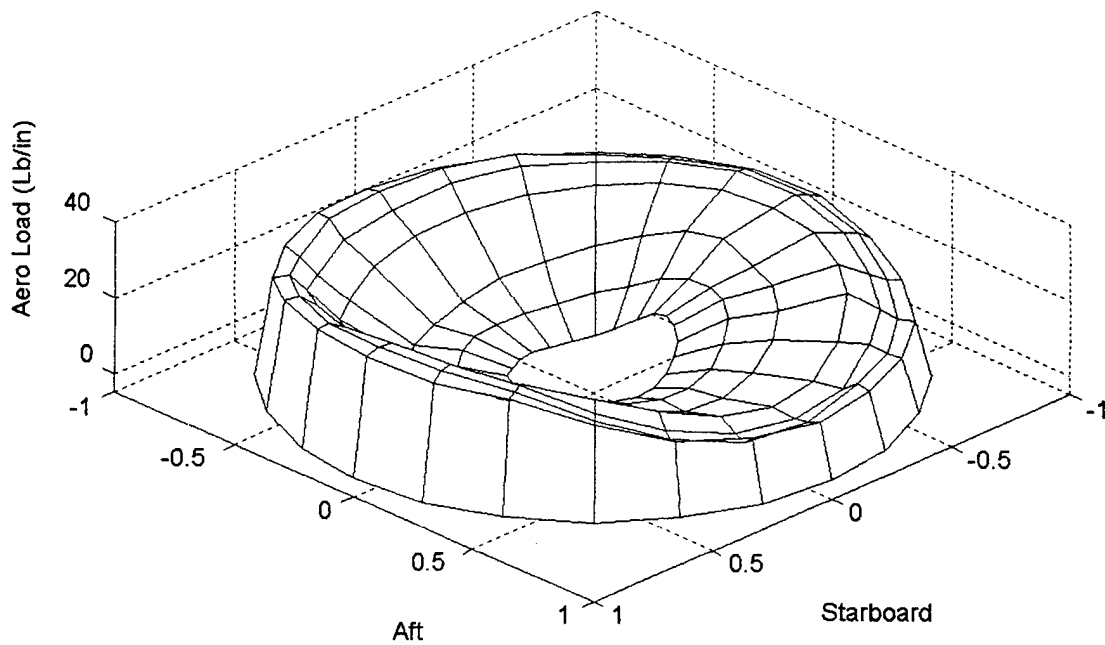
Figure 21. H-34 Airload Distribution at 115 Kts - Flight.
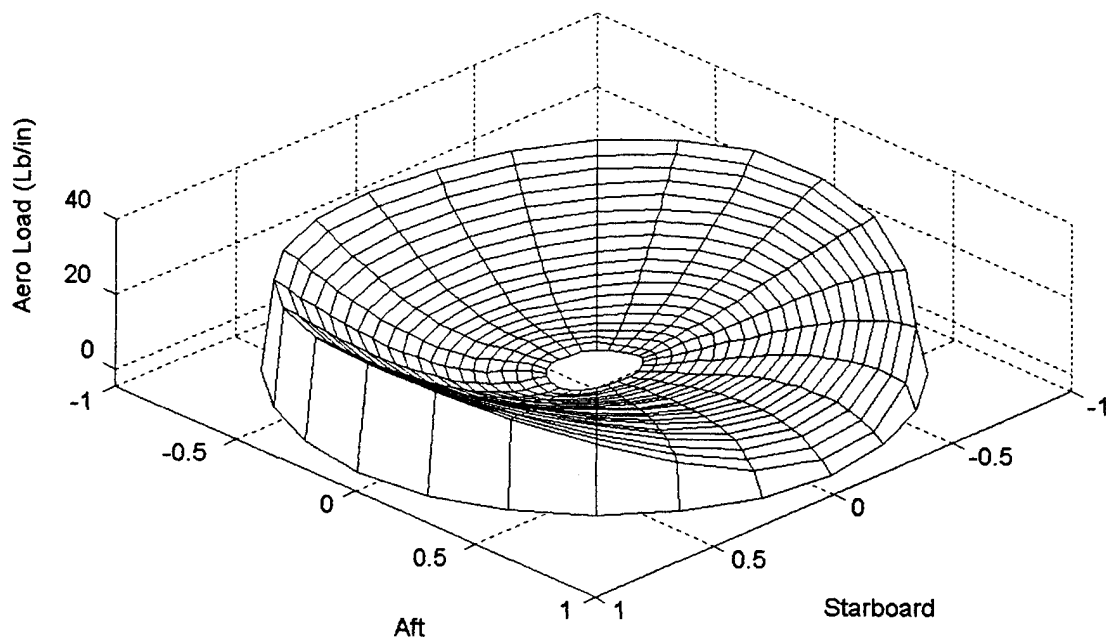
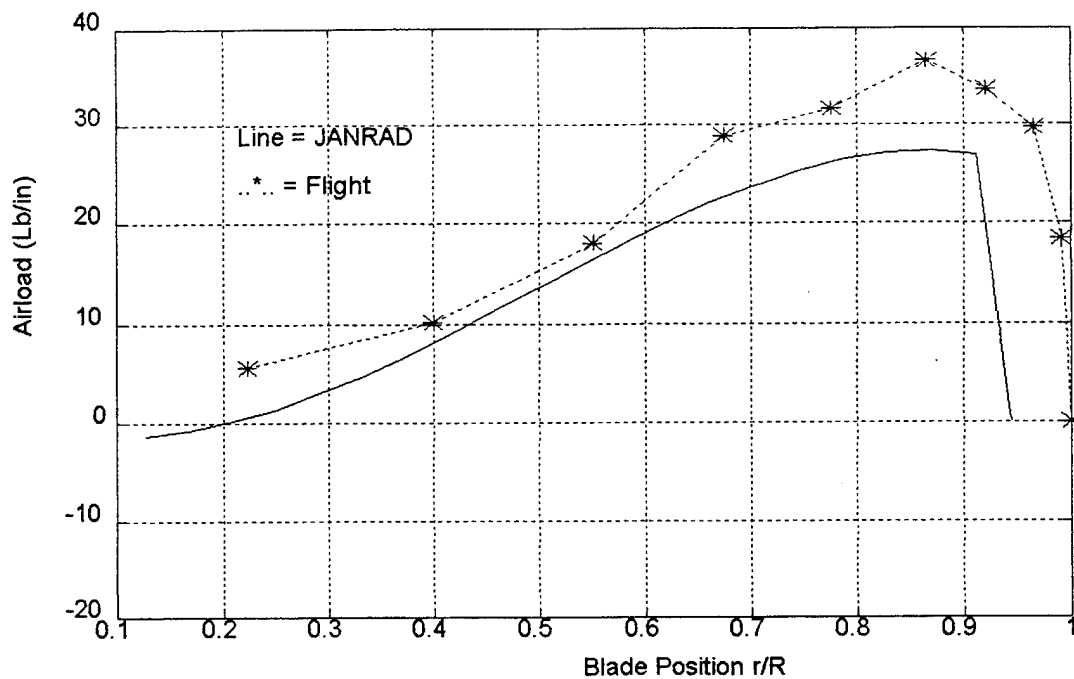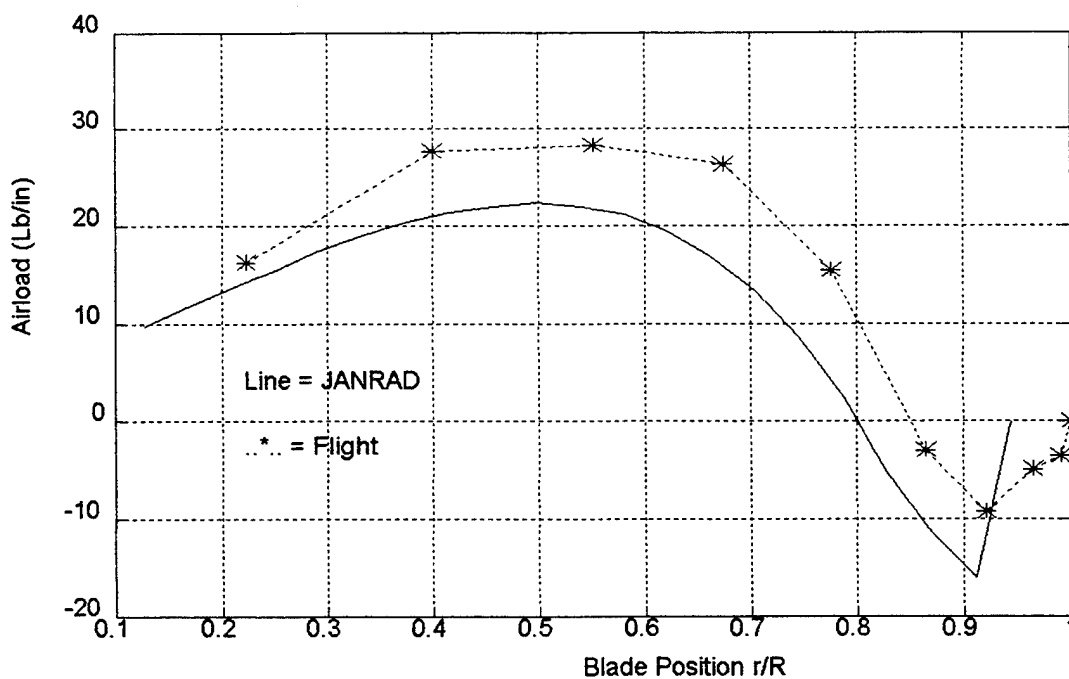**Figure 22.** H-34 Airload Distribution at 115 Kts - JANRAD.

47
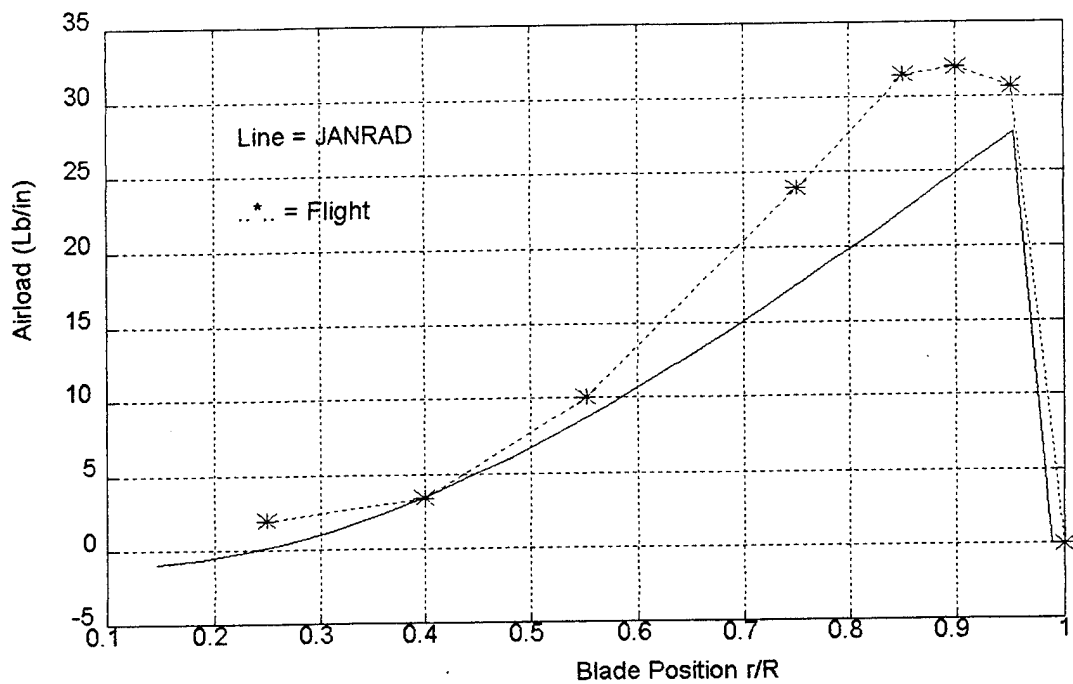
Figure 23. H-34 Radial Airload Distribution at 115 Kts, $\Psi = 0^\circ$.
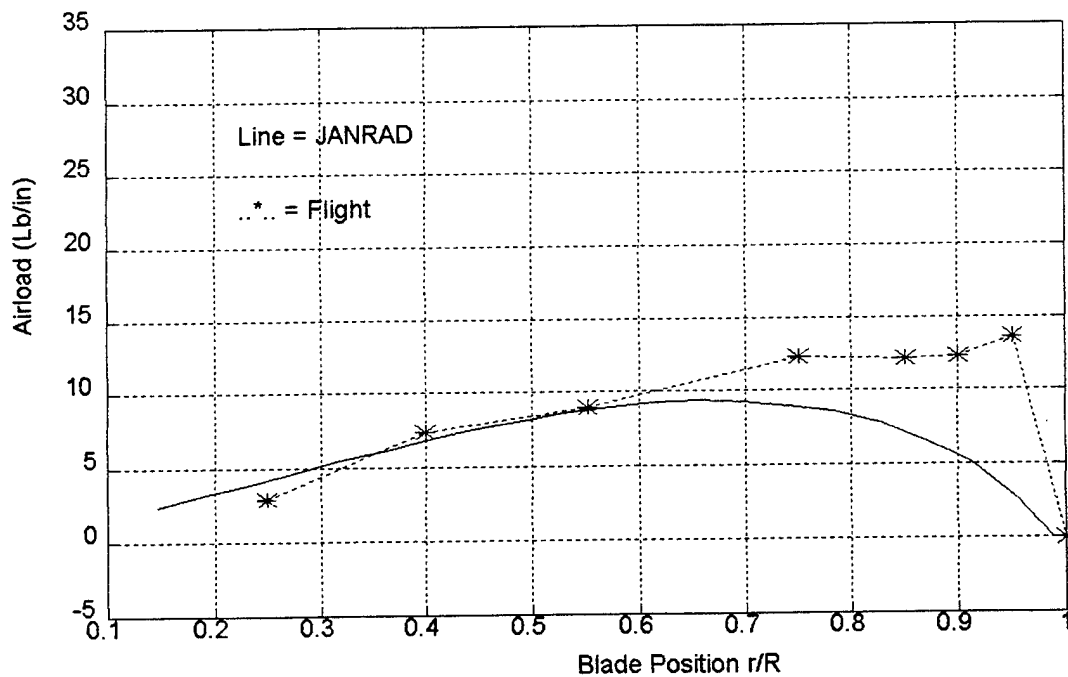
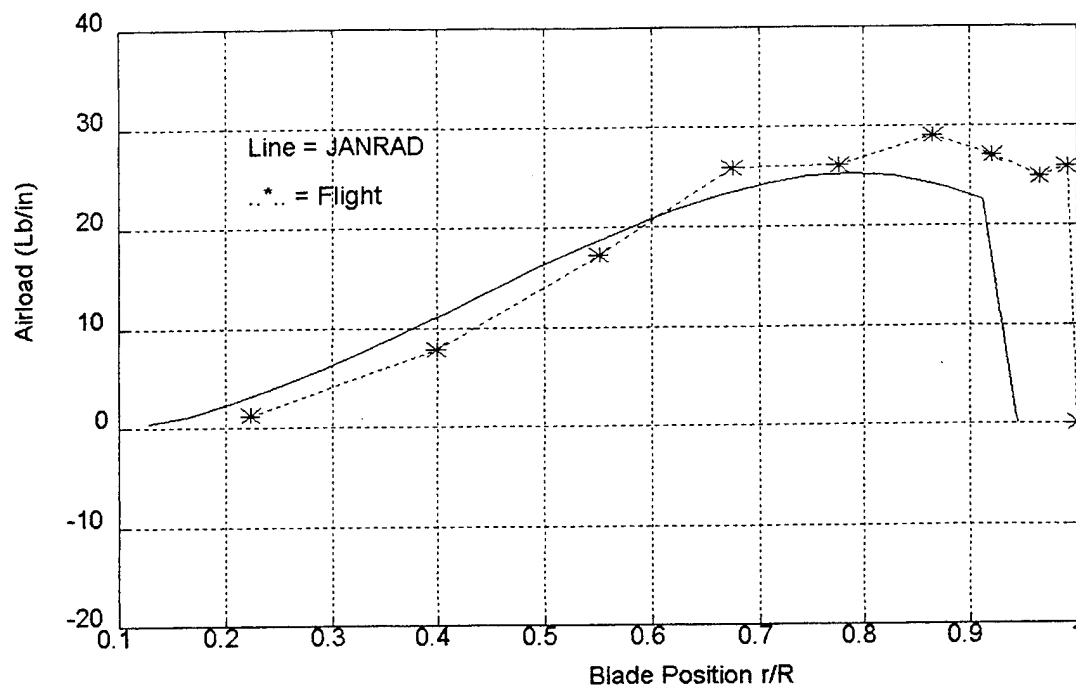**Figure 24.** H-34 Radial Airload Distribution at 115 Kts, $\Psi = 90^\circ$.

48
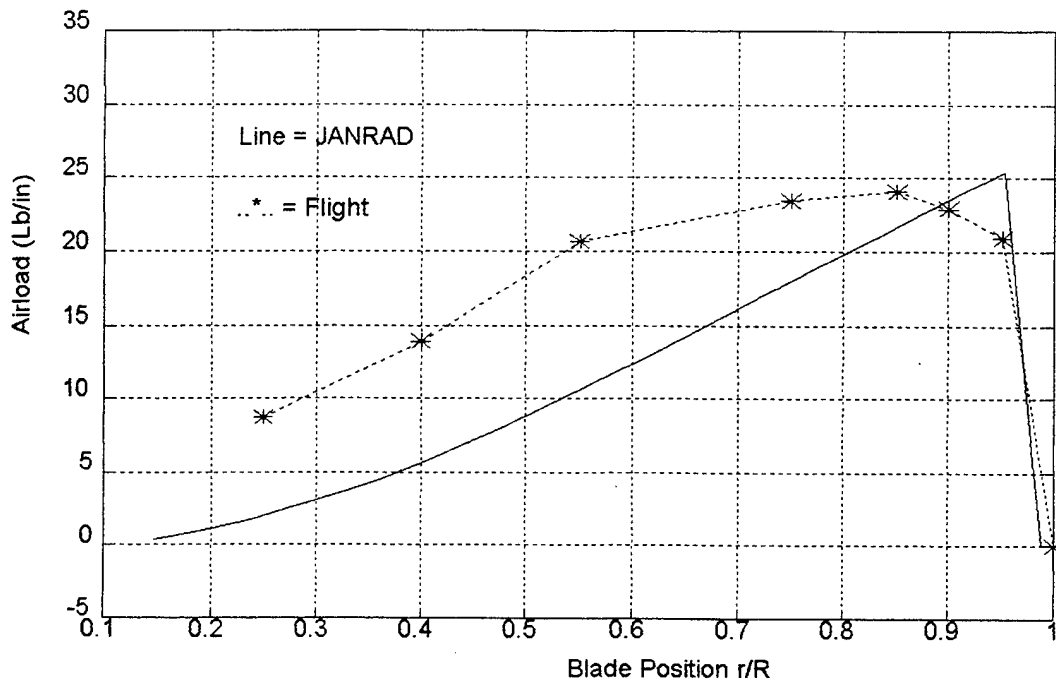
Figure 25. H-34 Radial Airload Distribution at 115 Kts, $\Psi = 180°$.
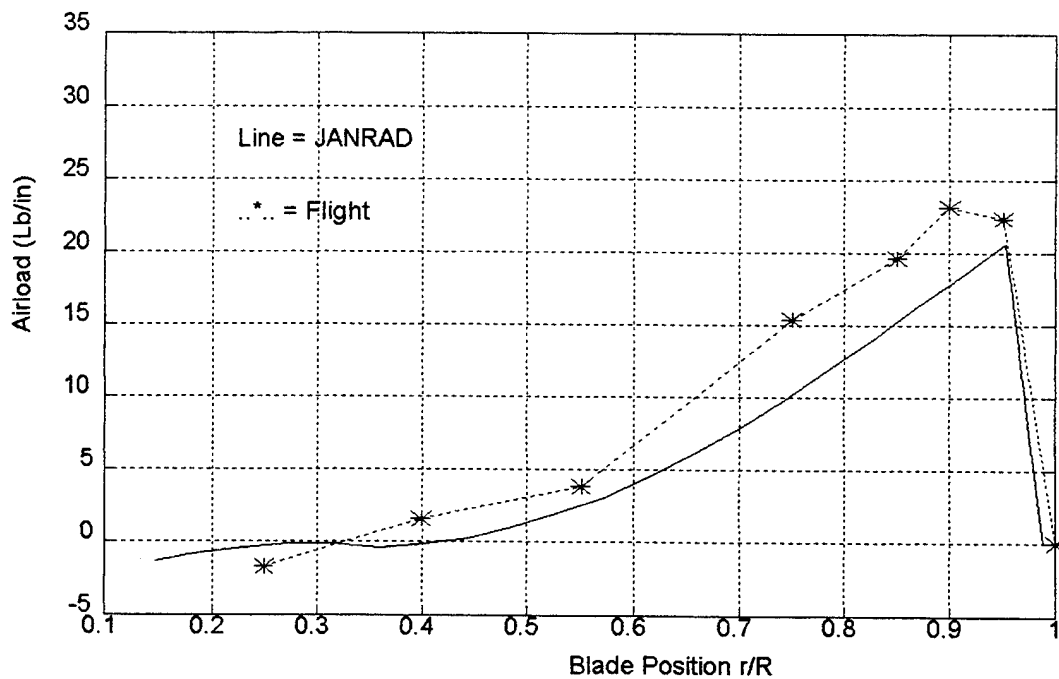
Figure 26. H-34 Radial Airload Distribution at 115 Kts, $\Psi = 270°$.

49
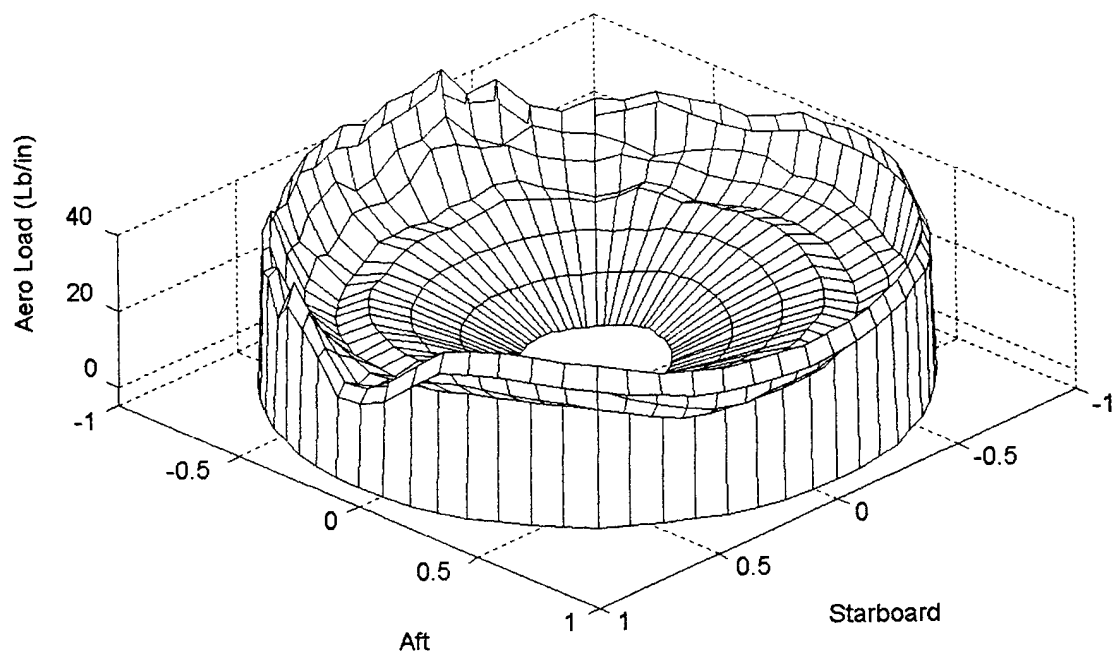
Figure 27. UH-60A HOGE Airload Distribution - Flight
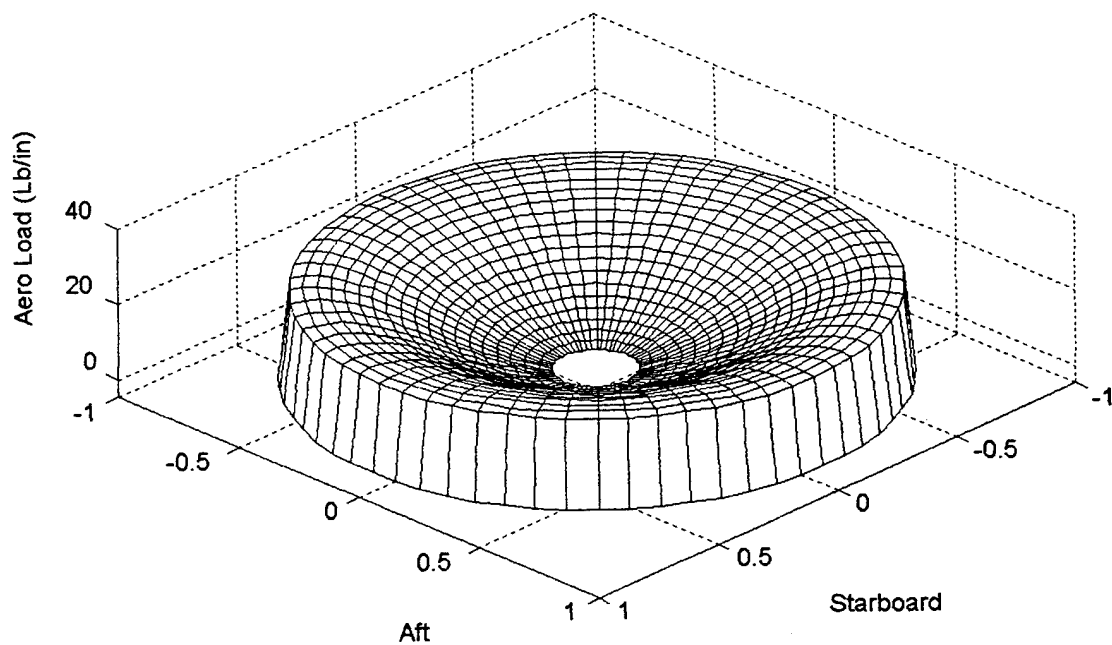
Figure 28. UH-60A HOGE Airload Distribution - JANRAD
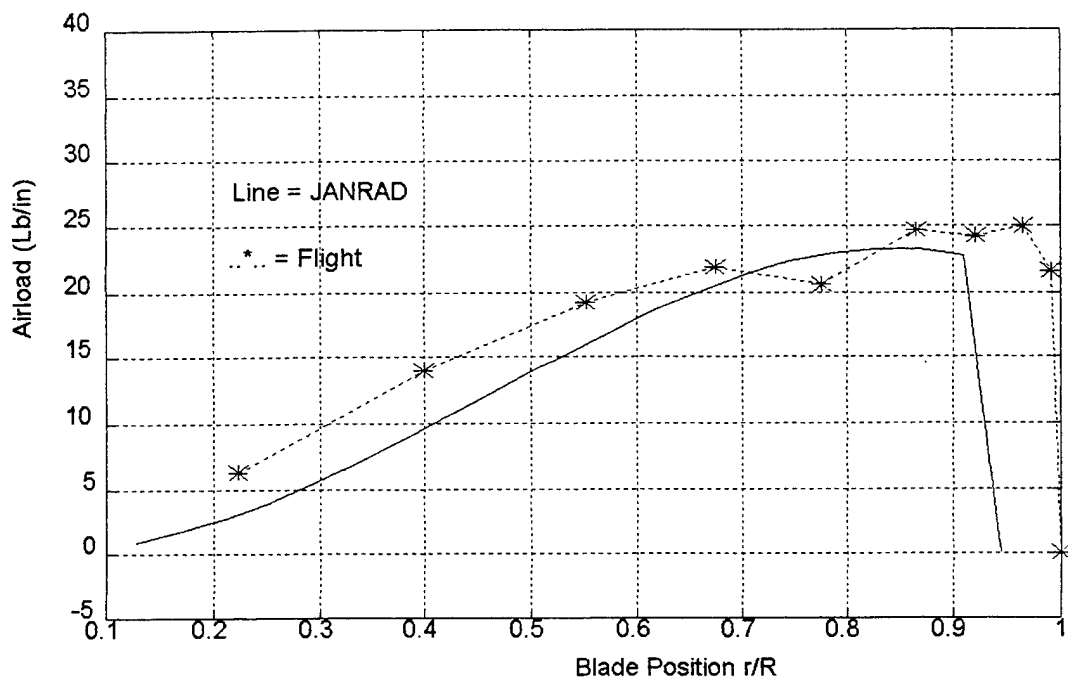
Figure 29. UH-60A Radial Airload Distribution, HOGE, $\Psi = 0°$.
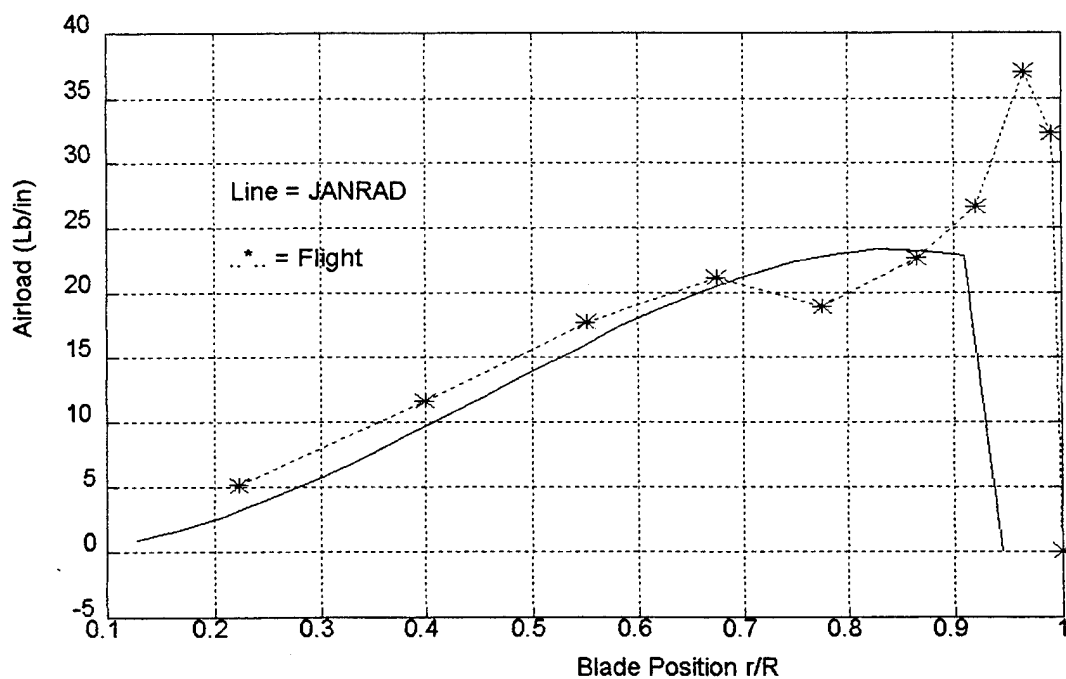
Figure 30. UH-60A Radial Airload Distribution, HOGE, $\Psi = 90°$.
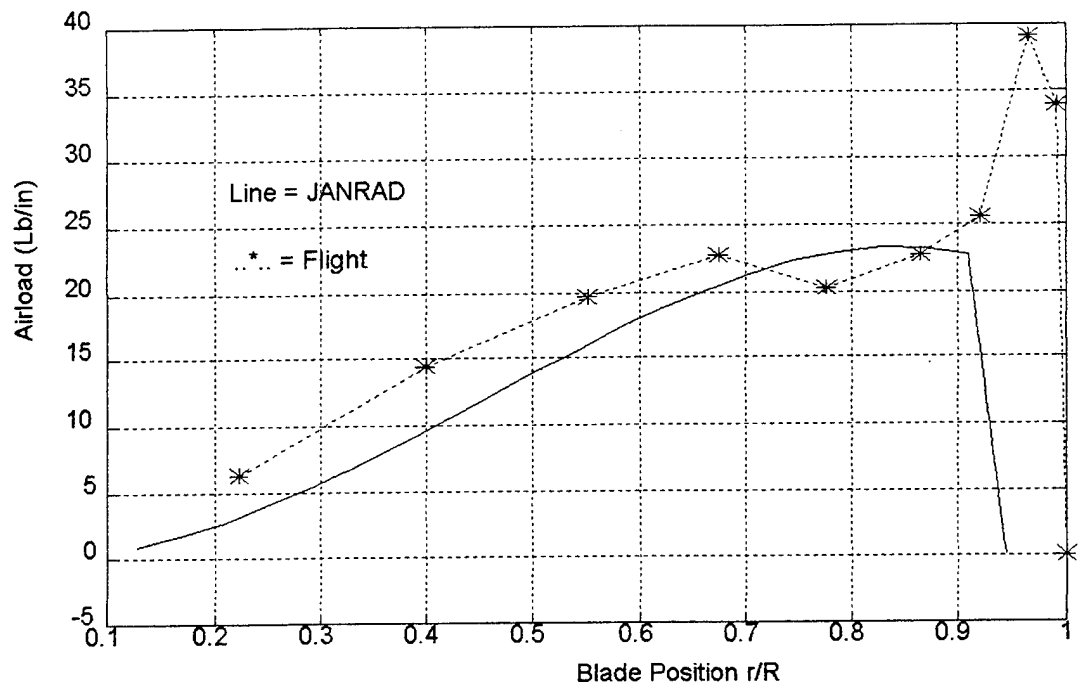
Figure 31. UH-60A Radial Airload Distribution, HOGE, $\Psi = 180°$.
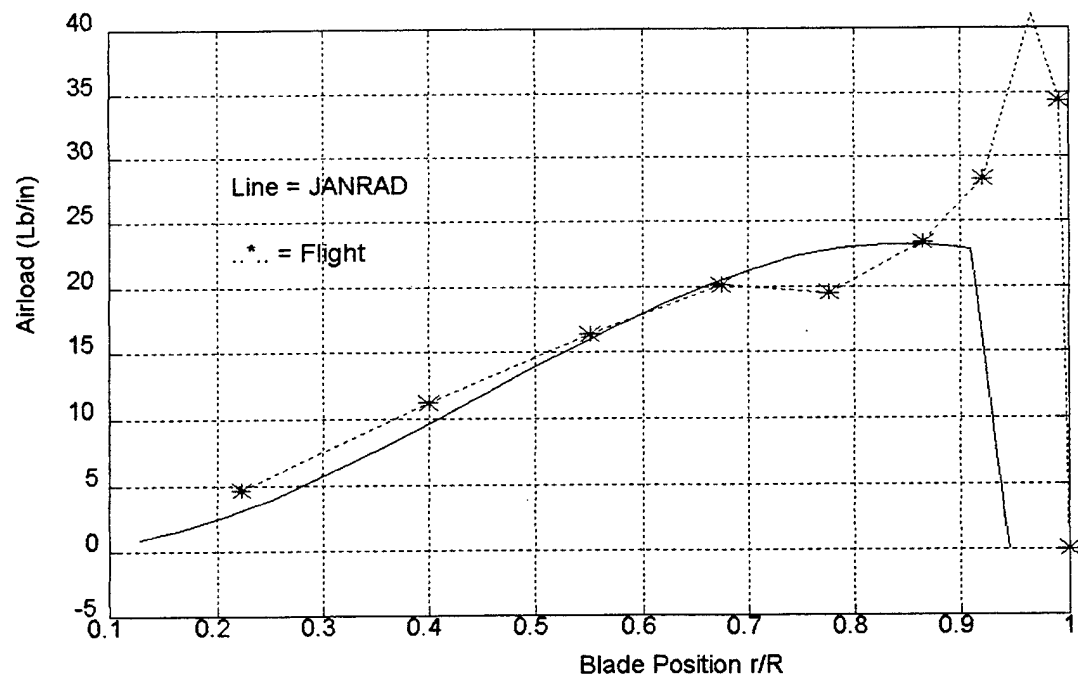
Figure 32. UH-60A Radial Airload Distribution, HOGE, $\Psi = 270°$.
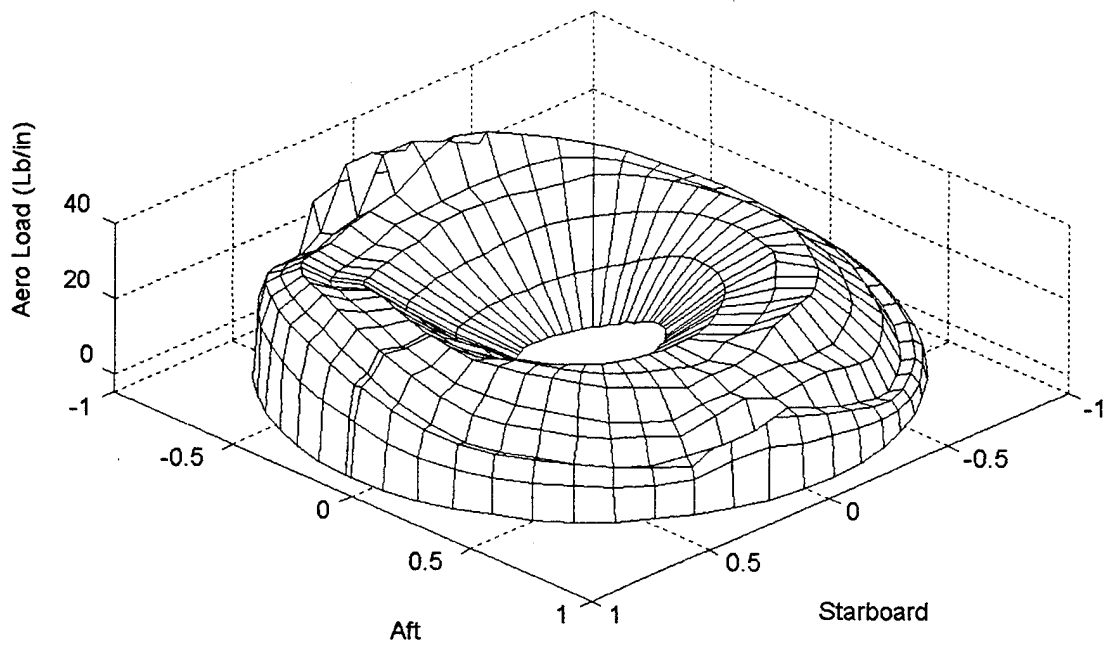
Figure 33. UH-60A Airload Distribution at 65 Kts - Flight.
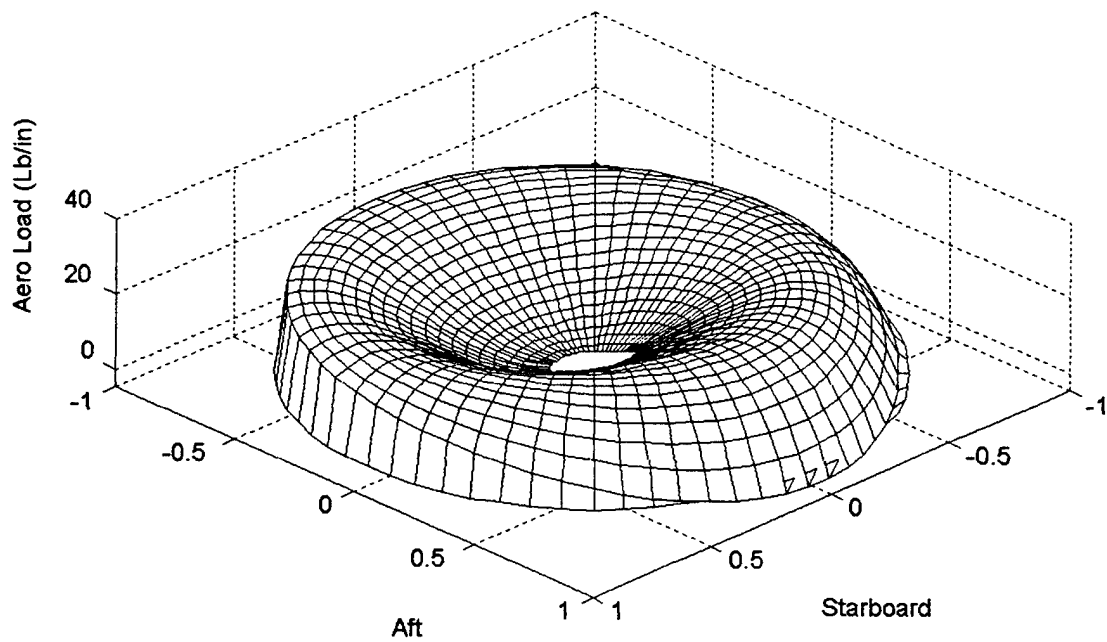
Figure 34. UH-60A Airload Distribution at 65 Kts - JANRAD.

53
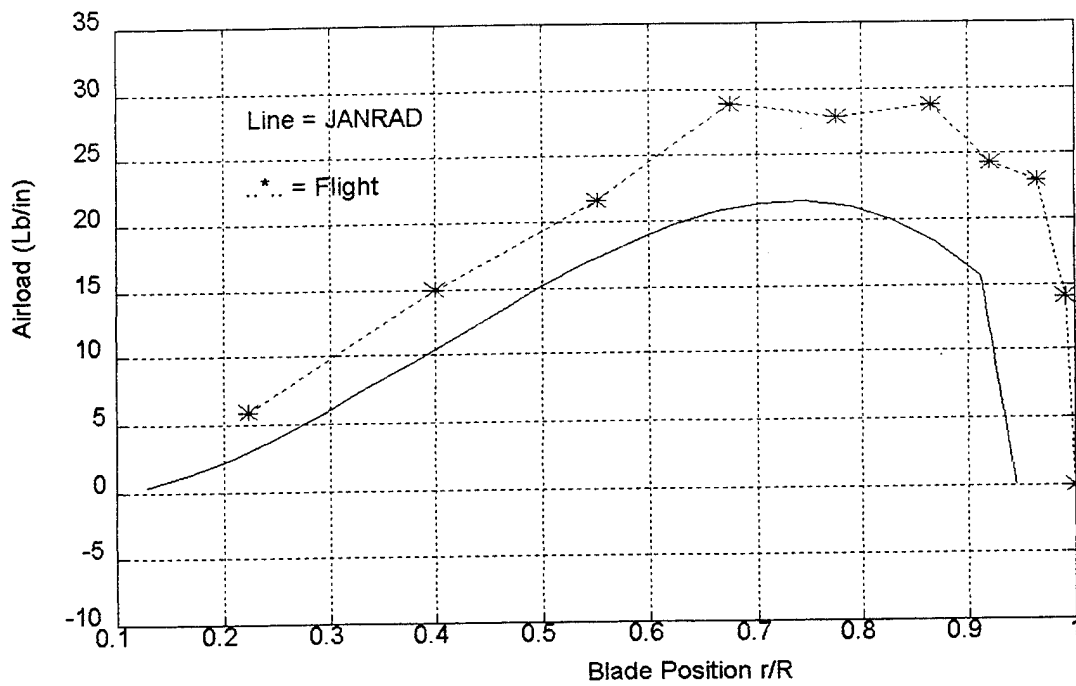
Figure 35. UH-60A Radial Airload Distribution at 65 Kts, $\Psi = 0^\circ$.
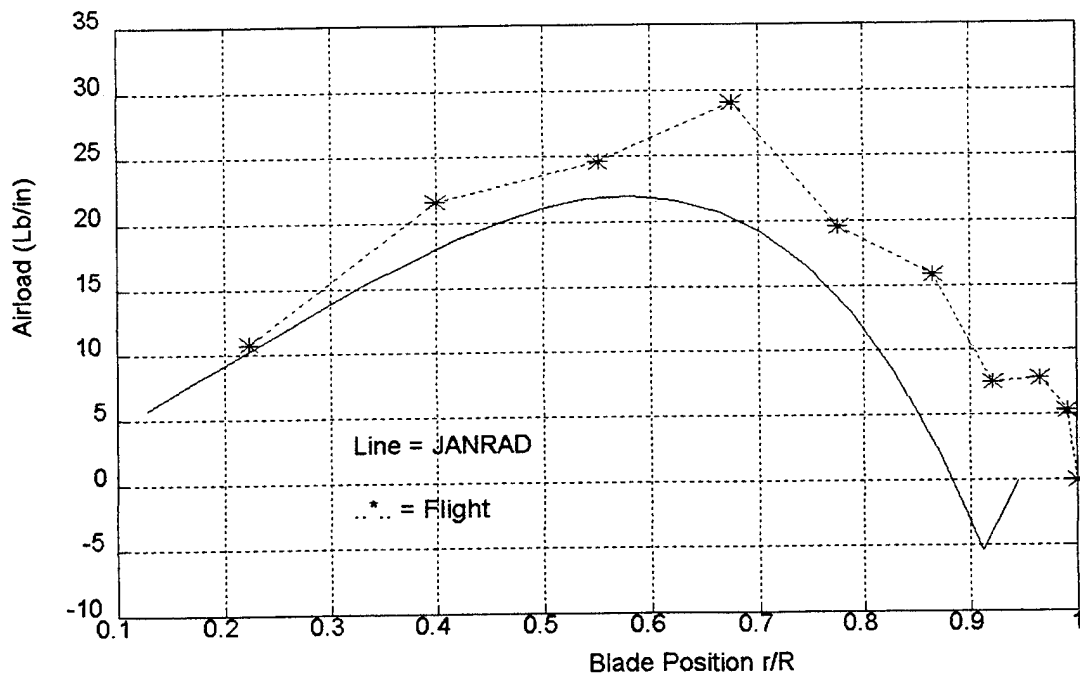
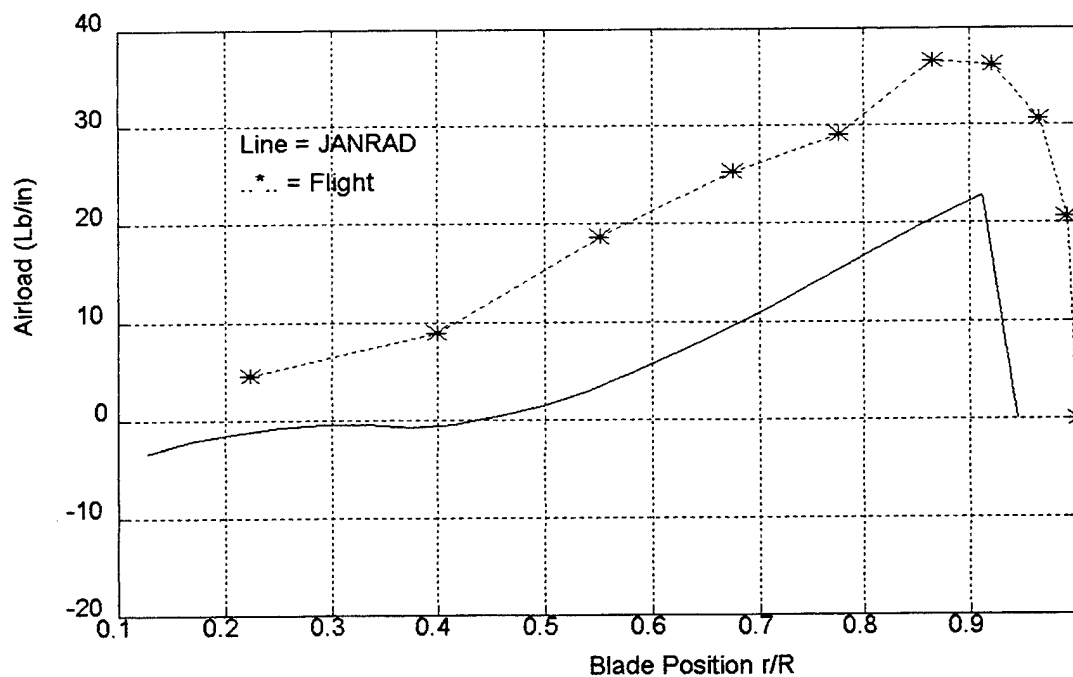**Figure 36.** UH-60A Radial Airload Distribution at 65 Kts, $\Psi = 90^\circ$.

Figure 37. UH-60A Radial Airload Distribution at 65 Kts, $\Psi = 180°$.

Figure 38. UH-60A Radial Airload Distribution at 65 Kts, $\Psi = 270°$.

55

Figure 39. UH-60A Airload Distribution at 115 Kts - Flight.

Figure 40. UH-60A Airload Distribution at 115 Kts - JANRAD.

56

Figure 41. UH-60A Radial Airoad Distribution at 115 Kts, $\Psi = 0°$.

Figure 42. UH-60A Radial Airload Distribution at 115 Kts, $\Psi = 90°$.

57

Figure 43. UH-60A Radial Airload Distribution at 115 Kts, $\Psi = 180°$.

Figure 44. UH-60A Radial Airload Distribution at 155 Kts, $\Psi = 270°$.

APPENDIX G. POWER REQUIRED FIGURES
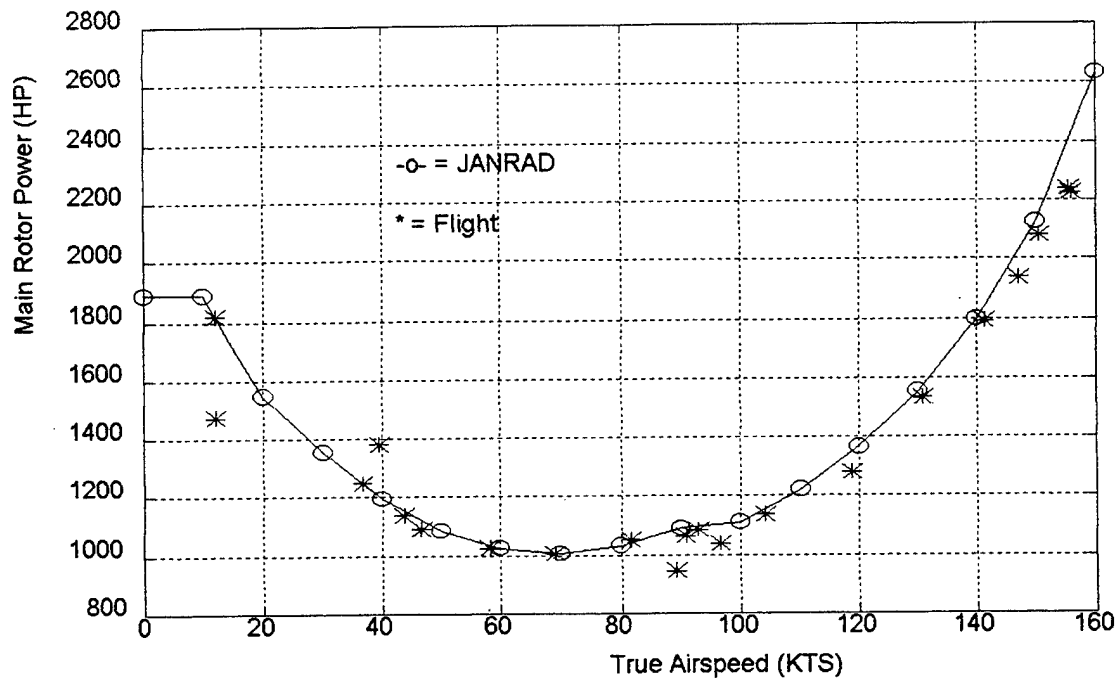
Figure 45. UH-60A Power Required vs Airspeed, Flight #84.
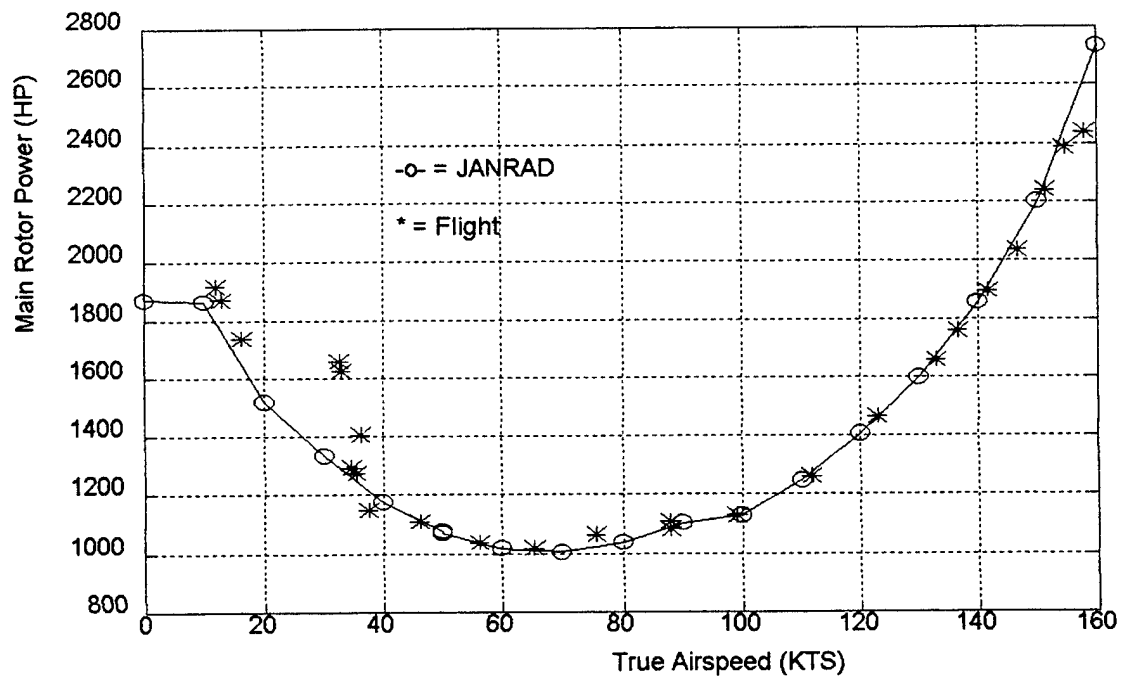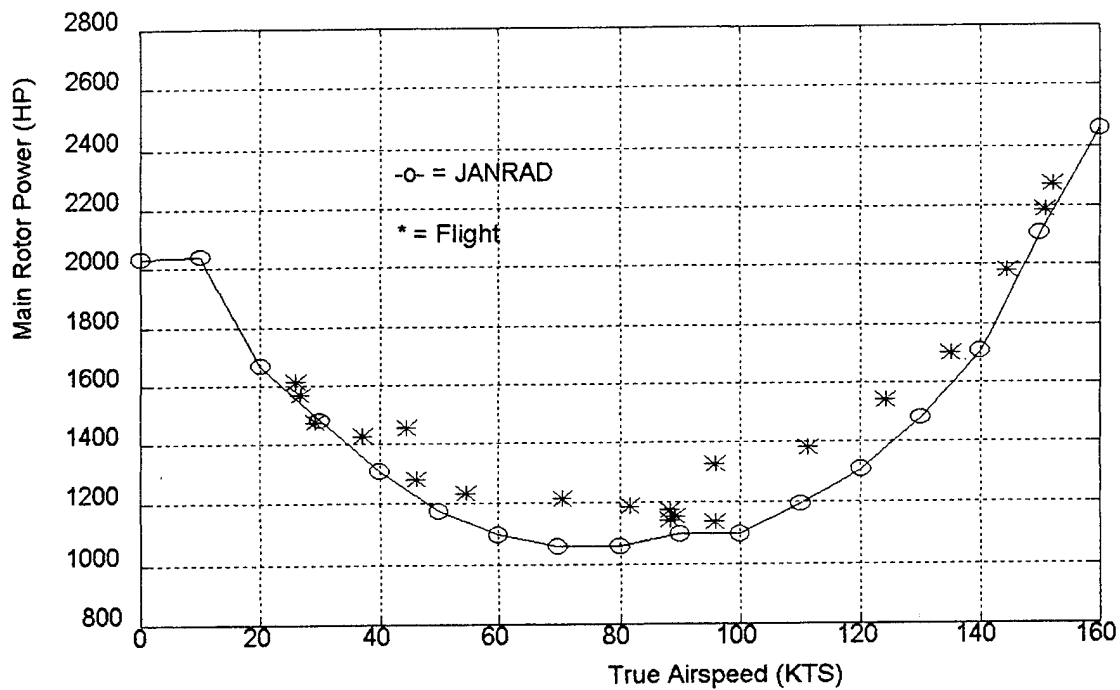

Figure 46. UH-60A Power Required vs Airspeed, Flight #85.

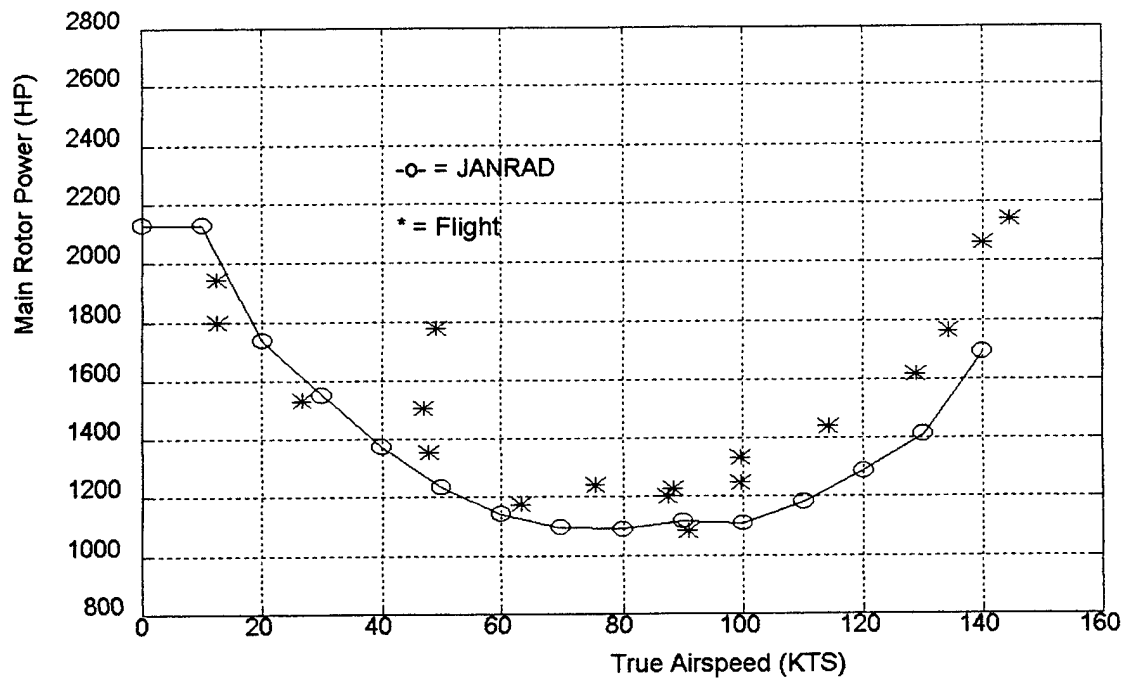**Figure 47.** UH-60A Power Required vs Airspeed, Flight #88.

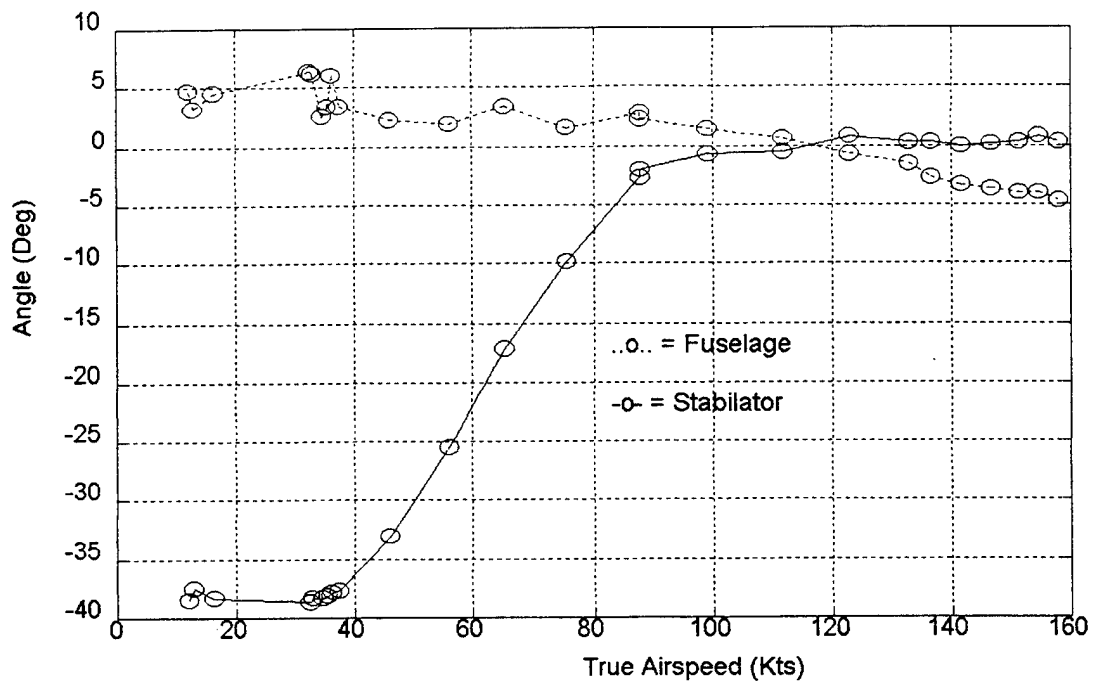**Figure 48.** UH-60A Power Required vs Airspeed, Flight #89.

60

Figure 49. UH-60A Stabilator and Fuselage Position, Flight #85.

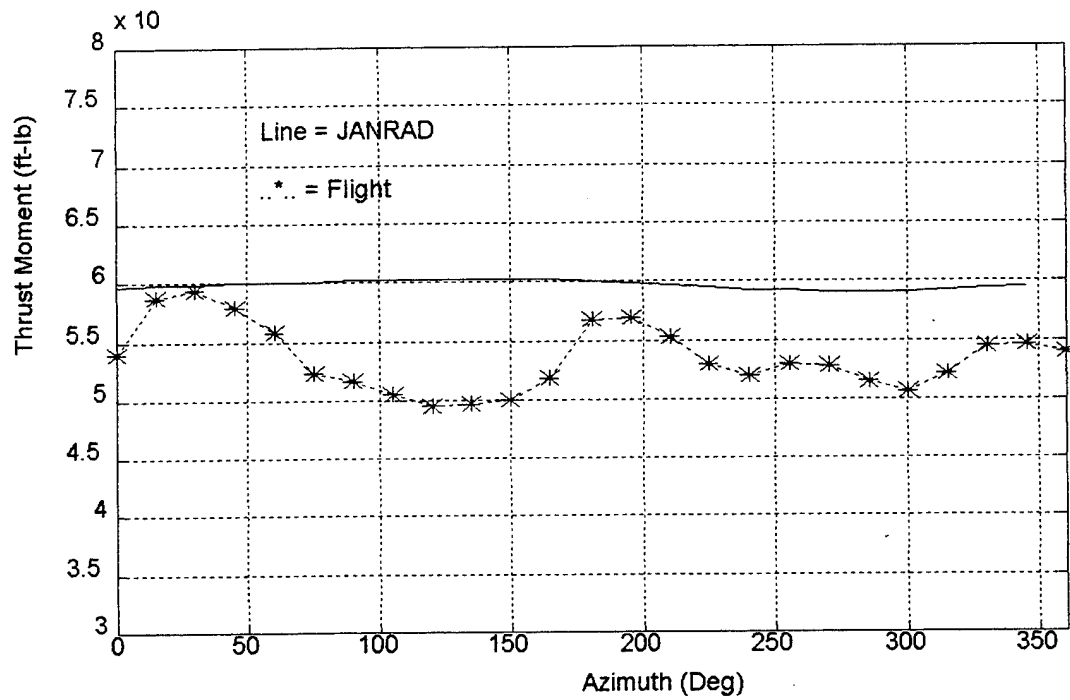# APPENDIX H. THRUST MOMENT FIGURES

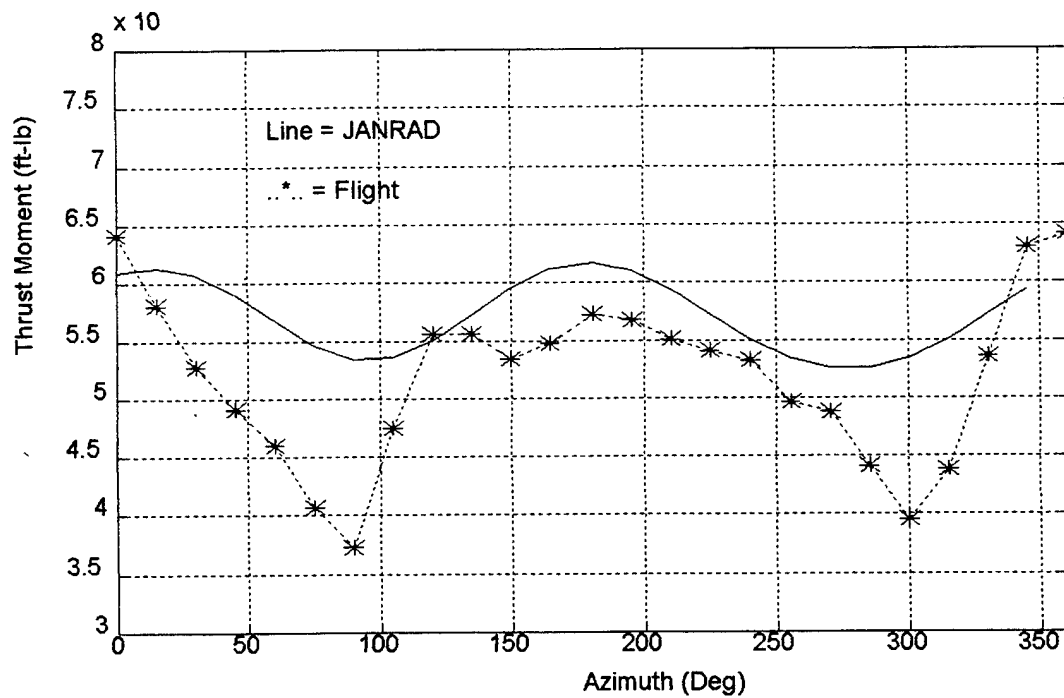**Figure 50.** H-34 HOGE Thrust Moment Variation with Azimuth.

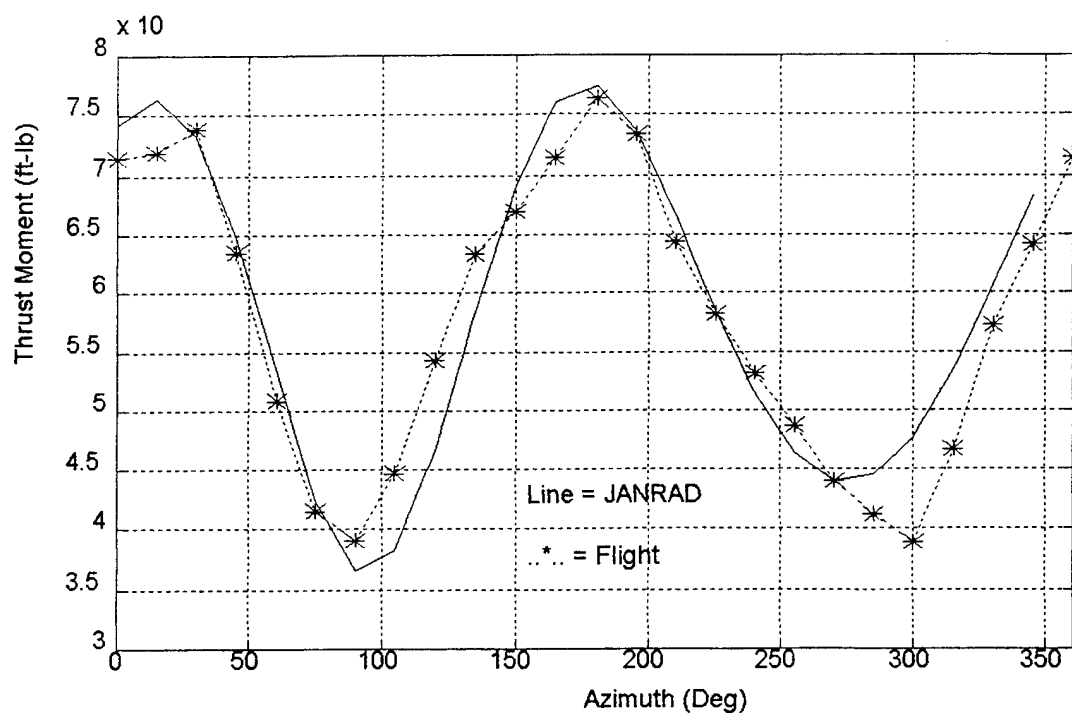**Figure 51.** H-34 Thrust Moment Variation with Azimuth at 56 Kts.

63.

Figure 52. H-34 Thrust Moment Variation with Azimuth at 115 Kts.
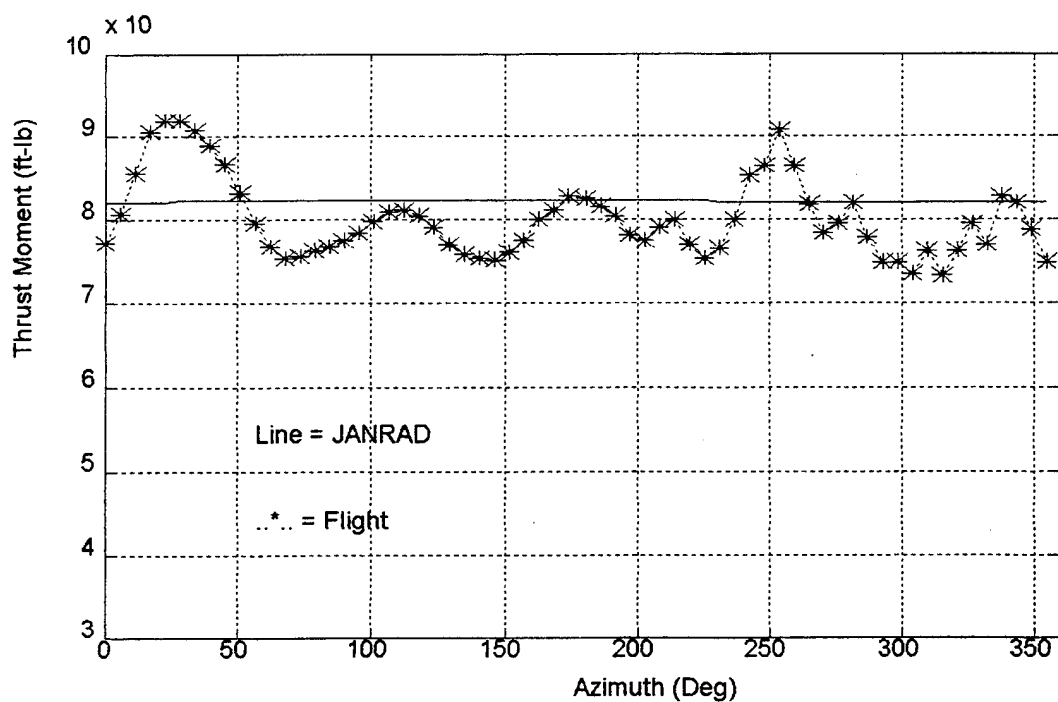

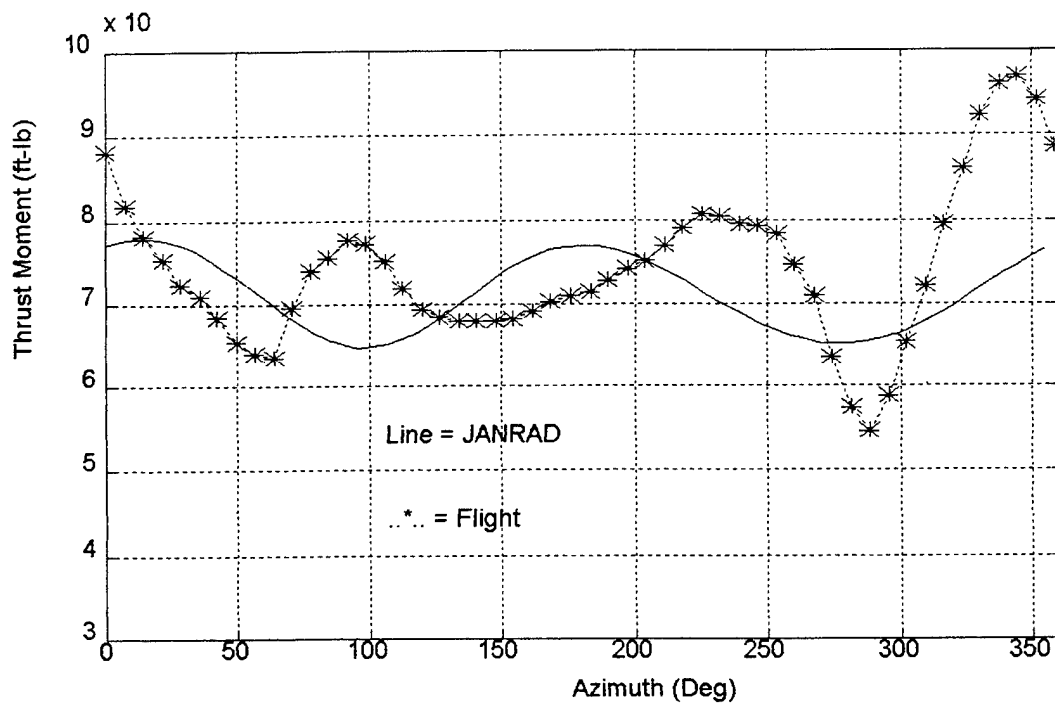**Figure 53.** UH-60A HOGE Thrust Moment Variation with Azimuth.

64

Figure 54. UH-60A Thrust Moment Variation with Azimuth at 65 Kts.
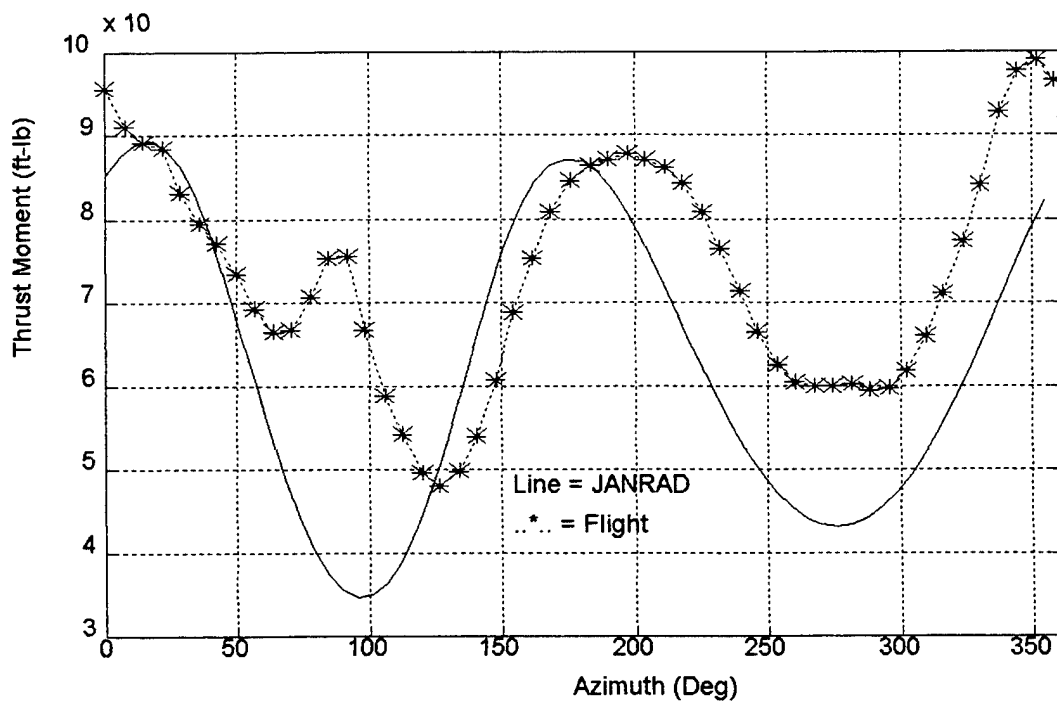

Figure 55. UH-60A Thrust Moment Variation with Azimuth at 115 Kts.

65

LIST OF REFERENCES

1   Nicholson, R. K. Jr., *Computer Code for Interactive Rotorcraft Preliminary Design Using a Harmonic Balance Method for Rotor Trim*, Naval Postgraduate School, Thesis for MSAE Degree, Monterey, CA, 1993.

2   Wirth, W. M. Jr., *Linear Modeling of Rotorcraft for Stability Analysis and Preliminary Design*, Naval Postgraduate School, Thesis for MSAE Degree, Monterey, CA, 1993.

3   Scheiman, J., *A Tabulation of Helicopter Rotor-blade Differential Pressures, Stresses, and Motions as Measured in Flight*, NASA Technical Memorandum TM X-952, 1964.

4   Bondi, M. J. and Bjorkman, W. S., *TRENDS, A Flight Test Relational Database User's Guide and Reference Manual*, NASA Technical Memorandum 108806, 1994.

5   Wood, E. R., Kolar, R. and Cricelli, A. S., "A Time Dependent Tip Loss Formula for Rotor Blade Dynamic Analysis", *Seventeenth European Rotorcraft Forum*, Paper No. 91 - 57, 1991.

6   Prouty, R. W., *Helicopter Performance, Satbility, and Control*, Krieger Publishing, 1990.

7   Schlichting, H., *Boundary Layer Theory*, McGraw - Hill, 1960.

8   Gerstenberger, W. and Wood, E.R., "Analysis of Helicopter Aeroelastic Characteristics in High-Speed Flight", *AIAA Journal*, Vol. 1, No. 10, pp. 2366-2381, November 1963.

INITIAL DISTRIBUTION LIST

1. Defense Technical Information Center   2
    Cameron Station
    Alexandria, Virginia 22304 - 6145

2. Library, Code 52   2
    Naval Postgraduate School
    Monterey, California 93943 - 5000

3. Professor Daniel J. Collins, Code AA/Co   1
    Department of Aeronautics and Astronautics
    Naval Postgraduate School
    Monterey, California 93943 - 5000

4. Professor E. Roberts Wood, Code AA/Wd   4
    Department of Aeronautics and Astronautics
    Naval Postgraduate School
    Monterey, California 93943 - 5000

5. Professor S.K. Hebbar, Code AA/Hb   1
    Department of Aeronautics and Astronautics
    Naval Postgraduate School
    Monterey, California 93943 - 5000

6. LT David M. Eccles USN   1
    1240 Grand Avenue
    San Diego, California 92109

7. MAJ Robert K. Nicholson, Jr. USA   1
    1116 Walker Road
    Great Falls, Virginia 22066

8. MAJ Walter M. Wirth   1
    P.O. Box 11282
    Burke, Virginia 22009 - 1282

9. Dr. Dev Bannerjee   1
    1102 Hackamore Street
    Mesa, Arizona 85203

10.	Mr. William G. Bousman NASA Ames Research Center M/S 215 - 1 Moffett Field, California 94035	1
11.	Mr. Dean Carico Star Route, Box 175 Ridge, Maryland 20680	1
12.	Dr. Raymond G. Carlson 140 New Haven Avenue Orange, Connecticut 06477	1
13.	Mr. Dean R. Cooper 85 Golden Hill Trumbull, Connecticut 06611	1
14.	Mr. Charles C. Crawford 1220 Winding Branch Circle Dunwoody Atlanta, Georgia 30338	1
15.	Mr. Leo Dadone 298 Summit House West Chester, Pennsylvania 19380	1
16.	Professor Alfred Gessow University of Maryland Department of Aerospace Engineering College Park, Maryland 20742	1
17.	Mr. Robert D. Hubbard 151 Shaelah Court St. Charles, Missouri 63033	1
18.	Mr. Henrey L. Kelley 3092 North Riverside Drive Lanexa, Virginia 23089	1
19.	Mr. Andrew W. Kerr 21950 McKean Road San Jose, California 95120	1

20.	Dr. Andrew Z. Lemnios Rensselaer Polytechnic Institute JEC 4010 Troy, New York 12180	1
21.	Dr. Robert G. Loewy School of Aerospace Engineering Georgia Institute of Technology Atlanta, Georgia 30332 - 0150	1
22.	Mr. John C. McKeown 315 Braehead Drive Fredericksburg, Virginia 22401	1
23.	Dr. Robert A. Ormiston NASA Ames Research Center M/S 215 - 1 Moffett Field, California 94035	1
24.	Mr. Raymond W. Prouty 4224 Deerpark Court Westlake Village, California 91361	1
25.	Dr. Fredric H. Schmitz 3872 Dixon Place Palo Alto, California 94305	1
26.	Dr. Michael P. Scully P.O. Box 1120 Mountain View, California 94042	1
27.	Dr. John Shaw 655 Newlin Road Springfield, Pennsylvania 19064	1
28.	Dr. Robert E. Singleton United States Army Research Office Box 12211 Research Triangle Park, North Carolina 27709	1
29.	Dr. Roger L. Smith 1958 East Ranch Road Tempe, Arizona 85284	1

30. Dr. Frederich K. Straub   1
    1760 East Halifax Street
    Mesa, Arizona 85203

31. Dr. William Warmbrodt   1
    NASA Ames Research Center
    M/S T12 - B
    Moffett Field, California 94035

32. Dr. Jing G. Yen   1
    1812 Lakemont Court
    Arlington, Texas 76013